OFFICE OF NAVAL RESEARCH
Contract Nonr 982-(04)
Task No. NR 031 - 611

FINAL REPORT

GRAIN BOUNDARY DIFFUSION IN LEAD

by

J. P. Stark and W. R. Upthegrove

UNIVERSITY OF OKLAHOMA RESEARCH INSTITUTE
Norman, Oklahoma

31 May 1963

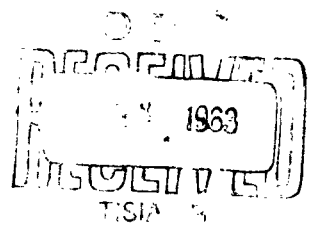

OFFICE OF NAVAL RESEARCH

Contract Nonr 982-(04)

Task No. NR 031-611

FINAL REPORT

GRAIN BOUNDARY DIFFUSION IN LEAD

by

J. P. Stark and W. R. Upthegrove

THE UNIVERSITY OF OKLAHOMA RESEARCH INSTITUTE

Norman, Oklahoma

31 May 1963

GRAIN BOUNDARY DIFFUSION IN LEAD*

ABSTRACT

The purpose of this research was to investigate grain boundary self-diffusion in high purity lead and, specifically, to study the influence of orientation and impurity content upon this phenomena.

Bicrystals of zone-refined lead were grown from the melt with various tilt and twist grain boundary orientations to study the effect of misfit. For the study of impurity effects, bicrystals with similar misfit were grown with lead containing varying amounts of the impurities tin, thallium, indium, and bismuth.

Diffusion experiments were carried out using high resolution autoradiography and lead-210. Diffusion coefficients were determined from the Whipple and Fisher diffusion models with the data of depth of penetration measurements. These diffusion coefficients varied between 5.1×10^{-8} and 4.0×10^{-6} centimeters squared per second with the Whipple model. The

---

*This report presents the material submitted by J. P. Stark as a dissertation to the Graduate Faculty of the University of Oklahoma in partial fulfillment of the requirements for the degree of Doctor of Philosophy.

activation energy for grain boundary diffusion demonstrated a decrease from the lattice diffusion activation energy of about 25 kilocalories per mole to 5.5 kilocalories per mole for a grain boundary with 30 degrees of misfit. Also, in this misfit range, the ratio of grain boundary diffusivity to that of the lattice varied between 10^4 and 10^8.

The impurity study resulted in the observation of a 50 per cent decrease in the grain boundary self-diffusion coefficient of lead in a 30 degree tilt grain boundary with increasing concentrations of tin, thallium, and indium. Radioactive lead penetration of bismuth alloys was not observed. This was attributed to the lack of adherence of the active electroplate and was caused by oxidation of bismuth. The activation energy for grain boundary diffusion decreased slightly with increasing impurity contents

INDEX OF TECHNICAL REPORTS

Report Number	Date
1	15 February 1958
2	15 February 1959
3	15 February 1960
4	15 February 1961
5	15 February 1962

INDEX OF PUBLICATIONS

No publications have been made in connection with the work performed under this contract.

FOREWARD

This report is based on a dissertation submitted by John P. Stark to the Graduate Faculty of the University of Oklahoma in partial fulfillment of the requirements for the degree of Doctor of Philosophy. This investigation was supported by the Office of Naval Research under Contract Nonr 982(04), Task No. NR 031-611.

The authors, John P. Stark (former Research Assistant, University of Oklahoma Research Institute) is presently Assistant Professor, School of Mechanical Engineering, The University of Texas, and W. R. Upthegrove (former Associate Professor and Chairman, School of Metallurgical Engineering, The University of Oklahoma) is currently associated with International Nickel Company.

TABLE OF CONTENTS

LIST OF TABLES

LIST OF ILLUSTRATIONS

GRAIN BOUNDARY DIFFUSION IN LEAD

CHAPTER I

INTRODUCTION

Grain Boundary Energy

A low angle symmetrical tilt grain boundary is pictured as being composed of equally spaced dislocations separated by regions of high strain energy. When the angle of misfit between the two crystals increases, the dislocations move closer together. Phenomenologically, the grain boundary can be thought of as a region where the interatomic spacing has, on the average, increased relative to the interatomic spacing in the crystal.

Strain energy can be associated with a region of material where the interatomic spacing is increased. The interatomic spacing is increased in a grain boundary, and therefore, a certain amount of strain energy can be associated with the crystal boundary surface. The grain boundary strain energy per unit area can be called a tension per unit length by a change of units. When three equilibrium grain boundaries meet, the tension in each boundary can be balanced by the angular relationship with which the grain boundaries

meet. Dunn and Lionetti (13) used this balance of forces and the angles with which three boundaries meet to arrive at an expression of the force balance.

$$\gamma_{kj}/\text{SIN } \theta_i = \text{Constant} ,$$

where γ_{kj} is the grain boundary tension between grains k and j and θ_i is the angle opposite this boundary, when three boundaries meet in a triad.

They proposed an experiment to measure the relative grain boundary energy by varying the misfit of one boundary and leaving the other two constant. Aust and Chalmers (4) used this precise method with tin tricrystals. For boundary angles less than six degrees the relative boundary energy increased almost linearly with misfit, however, for angles greater than ten degrees, the relative energy was constant.

Crussard, Friedel, and Cullity (12) used this same method to classify grain boundaries as to their relative energies. They found that a grain boundary between two random crystals contains almost a constant interfacial tension. If the two grains have a common crystallographic plane, the energy is less, and if the boundary were symmetrical, the energy is still lower. Finally, they determined that a twin boundary possesses almost zero energy.

Battner, Udin, and Wulff (6) introduced an experimental method whereby the absolute grain boundary energy can be determined. In it the crystal surface which the boundary meets is cleaned and highly polished. The bicrystal is then

submitted to a high temperature anneal (close to the melting point). Due to the tension in the grain boundary, a thermal groove is produced. The same geometrical force relationship holds except the grain boundary tension is balanced by the crystal surface tension. Thus if the crystal surface tension is known at the annealing temperature, the absolute grain boundary energy can be determined.

The theory of the grain boundary energy of a dislocation boundary was proposed by Read and Shockley (36). By stacking edge dislocations equally distant from one another, and summing the elastic strain energy interaction of single dislocations, they were able to arrive at an equation for the grain boundary energy.

$$T = \left[\frac{\mu a}{4\pi(1 - \nu)} \right] \theta \ (c - \mathrm{Ln}\ \theta) \ , \qquad (1)$$

where θ is the angle of boundary misfit, μ is the shear modulus, a is the lattice constant, and ν is Poisson's ratio. It is obvious that the use of elastic strains limits the applicability of equation 1 to small angles of misfit. However, qualitatively they expanded the theory of the boundary energy to include higher angles. In this argument they propose that certain orientations of grains produce smaller energies (energy cusps). Thus as θ varies, the grain boundary energy will have maxima followed by cusps. Read and Shockley justified this in that when a lattice plane is common to both grains of a symmetrical tilt boundary, the energy will be much lower.

It must be realized that this occurs when dislocations lie at integral numbers of lattice spacings from one another. Visualization of this can be accomplished by forming a grain boundary in a cubic metal from two grains aligned by the [100] direction. When this happens the (100) planes of the two grains are coplanar. Making a 28° boundary between the (010) planes of each grain produces a common (014) plane in each grain. With the same alignment of [100] directions and (100) planes, a 53° boundary about (010) planes produces a common (012) plane.

Gjostien and Rhines (18) used the previously mentioned experimental method of Battmer, Udin, and Wulff (6) to determine the absolute grain boundary energy in 99.95 per cent pure copper. In their work one finds that formula 6 is valid for very low grain boundary angles. Further, no energy cusps were observed. Fleischer (16), however, in discussing this work, explains the reasons no cusps were observed. He argued that a small amount of twist in a grain boundary changes the boundary energy, and further, small amounts of impurity content would lower the energy. With this lowering, the energy maxima could not be observed.

Another model for the strain energy of a boundary is presented by van der Merve (43). With the assumption that each grain is an elastic continuum, he treats dislocation models of twist and symmetrical tilt boundaries. MacKenzie (29), in a calculation of the interaction energy between two

square lattice planes, supports van der Merve. However, experimentally, van der Merve's model only holds for lower angles than Read and Shockley's. The basis for Fleischer's (16) argument of decreasing boundary energy with impurity content is a series of experiments starting with Stewart (38). Stewart added radioactive bismuth into lead, and used this alloy to grow a bicrystal. The segregation of bismuth to the bicrystal grain boundary during growth is observed by autoradiography. Nash (31) discussed Tipler's observations of the effect of antimony upon copper grain boundary energy observed by a dihedral angle technique. Antimony decreases the boundary energy from 600 ergs per square centimeter at 0 per cent to almost 200 ergs per square centimeter with 0.5 per cent added.

Belling and Winegard (7) studied the energy of coherent twin boundaries with and without silver added. In zone refined lead the relative energy is 0.050 ± 0.014, and with 0.1 per cent silver the energy is 0.077 ± 0.016.

The difference of these is most probably due to the fact that Tipler used an incoherent boundary where the amount of strain is decreased by the impurity addition. However, with the dense packing of the twin boundary, segregation increases the boundary strain. The important question arises, if the twin boundary is so densely packed that an impurity atom increases its energy, why does the impurity segregate at all? The answer probably lies in the number of possible impurity sites in the lattice. With 0.1 per cent silver, one

surmises that these are full, and to minimize the total crystal free energy, boundary sites would be the most probable even in the (210) twin boundary.

Thomas and Chalmers (40) studied segregation of polonium to the boundary of lead bicrystals. By varying the angle of misfit of bicrystals with common [100] grain directions, they concluded that the segregation is small and linear with misfit for angles less than 15°. Beyond 15° the segregation increases rapidly with misfit to the maximum angle of 25° studied. From this they conclude that at 15° dislocations begin to interact. By varying the annealing temperature, they further determine that the equilibrium segregation concentration in these low-angle boundaries decreases rapidly with temperature.

Grain Boundary Migration

A mechanistic approach to grain boundary migration follows from the manner with which atoms are able to migrate across the boundary. The velocity of such a process is necessarily controlled by the rate which these atoms are able to migrate from an equilibrium position in one crystalline grain across the grain boundary to a similar position in the adjoining grain. The atomic density an atom meets crossing the boundary would be less than that in the lattice. This atomic density should be about the same as an atom meets during migration down the boundary. This model would be a fair approximation in a material of high purity. However, in a

dilute binary alloy, one would not exactly correlate self-diffusion of the solvent or solute to boundary migration since migrating boundaries meet precipitated particles, inclusions, and so forth.

From an energy point of view, the amount of energy necessary per unit jump distance for an atom to cross the boundary should approximate the energy for an atom to migrate down the boundary in a very pure material. Also, melting is observed to nucleate at the boundary. Due to these basic ideas, Holmes and Winegard (26) are able to make comparisons between the free energies (ΔF) of activation for grain boundary self-diffusion, liquid self-diffusion, and boundary migration for some zone refined metals at their melting points.

The migration of two types of atoms through a grain boundary should be different than one type from an energy consideration. For this reason, it would be expected that the activation energy for boundary migration is concentration dependent. This dependence is observed by Gordon and Vandermeer (20) in an investigation of aluminum boundary migration with controlled amounts of copper. With 10^{-7} atom fraction copper, the migration activation energy is 15 kilocalories per gram mole. This energy increases to about 35 kilocalories per gram mole with 3×10^{-5} atom fraction copper.

Aust and Rutter (2, 3) have experimentally studied migration in zone refined lead crystals as a function of

orientation and contents of the impurities tin, silver, and gold. Their initial experimental work with tin demonstrated that the migration energy increases in random grain boundaries due to additions of tin. However, in orientated simple tilt boundaries, no change in activation energy was noted in the concentration range studied. This independence with concentration might follow from the fact that they did not use a constant boundary angle for the different concentrations. The boundary angles were an assemblage of different tilt angles between 22° and 48°. In the concentration range studied in the oriented boundaries, small inconsistent deviations in activation energy did occur; however, these were attributed to experimental error. In an initial examination, this seems justifiable, due to the larger energy changes in the migration of random grain boundaries.

Lattice Diffusion

It is impossible to analyze grain boundary diffusion without also considering lattice diffusion; therefore an understanding of lattice diffusion is desirable and necessary. The primary mechanism put forth to explain self- and substitutional solute diffusion in face centered cubic metals is the so-called vacancy mechanism. Other mechanisms have been theoretically studied and one excellent review of the lattice diffusion mechanisms is presented by LeClaire (28).

From a macroscopic point of view, lattice diffusion follows Fick's second law.

$$\frac{\partial C}{\partial t} = \nabla \cdot D\nabla C \ . \qquad (2)$$

This equation along with the assumption that D, the diffusion coefficient, is constant, form the basis for experimental determinations. Restricting this equation to one dimension and applying appropriate boundary conditions, such as

$$C\ (x,0) = 0$$

$$C\ (o,t) = C_o,$$

which are applicable when diffusion occurs from a constant concentration interface, yields the solution

$$C = C_o \left\{1 - \operatorname{erf} \frac{x}{2\sqrt{Dt}}\right\} \qquad (3)$$

where

$$\operatorname{erf}\ (\xi) = \frac{2}{\sqrt{\pi}} \int_o^{\xi} e^{-u^2}\, du.$$

Experimental self-diffusion data can be analysed by equation (3) when the labeled atoms are bonded to a single crystal; the crystal is annealed at a high temperature for a measured length of time, quenched and sectioned in thin slices to permit radiological analysis. Equation (3), along with the known experimental variables of concentration, distance, and time, determine a diffusion coefficient for the system at the temperature in question. Another diffusion determination at a different temperature yields a different value for D. Numerically these two diffusivities are related by the Arrhenius type equation.

$$D = D_o \exp\left(-\frac{Q}{Rt}\right) \qquad (4)$$

where Q is the activation energy for diffusion and D_o is the so-called frequency factor.

A physical interpretation of the activation energy lends insight to the diffusion problem. Its analysis must rely heavily on the mechanism by which diffusion occurs. Utilizing the vacancy mechanism, Hoffman and Turnbull (23) present a model describing solute diffusion in face-centered cubic metals. In this model the activation energy for diffusion of the ith component

$$Q^i = E_f^i + E_m^i \ , \tag{5}$$

where E_f^i is the energy to remove a nearest neighbor of an i type atom from the interior of the crystal to its surface, thereby creating an adjoining vacancy, and E_m^i is the energy expended in moving the i type atom into the vacancy. The binding energies between two solvent atoms and between a solvent and solute atom differ, therefore one expects that the activation energy for self-diffusion and solute diffusion differ. Hoffman and Turnbull's model predicts such a difference in activation energies. Available data are consistent with these predictions within the accuracies of the experiments.

Experimentally, Hoffman, Hart, and Turnbull (25) observed a change in the self-diffusion coefficient of silver when they introduce small solute additions of copper, lead, germanium, and aluminum. Hoffman and Turnbull (23) arrived

at an empirical equation for the diffusivity of copper which is linear with the mole fraction of lead added.

Further experimental evidence of concentration dependence is found by Resing and Nachtrieb (37). While studying the self-diffusion of lead with a radioactive lead isotope, they observe a change in the activation energy for self-diffusion when thallium is introduced. The study covered a spectrum of concentrations from zero to eighty seven per cent. The activation energy, 26.1 kilocalories per gram mole for pure lead, decreases to 24.5 kilocalories per gram mole with fifty per cent thallium present. This activation energy dependence on concentration is expected from equation (5).

Other thermodynamic variables also affect the activation energy. The effects of pressure on the self-diffusion of lead were studied by Hudson et al (27). Lead cylinders plated with radioactive lead-210, were annealed by a high temperature and pressure. Under the application of 40,000 kilograms per square centimeter, the activation energy increased from 25.0 kilocalories per gram mole to almost 28.0 kilocalories per gram mole. One expects this behavior because the energy for an atom's movement to a vacancy should increase due to the closer atomic packing when pressure is applied.

Pound, Bitler, and Paxton (34) have recently reviewed the kinetics of self-diffusion in body-centered cubic metals. They relate the diffusion coefficient D_o from equation (4), to the atomic jump direction, vibrational energy levels, and

entropy of activation. By a statistical mechanical analysis using absolute rate theory, they study self-diffusion in body-centered cubic metals, starting with

$$D_o = \alpha\, a^2\, \nu \exp\left(\frac{\Delta S}{R}\right), \qquad (6)$$

where α is determined by the geometry of atomic jumps, a is the lattice parameter, and ν is the Einstein vibrational frequency.

Grain Boundary Diffusion

In the 1930's, it was observed that diffusion is dependent on grain size; smaller grains increased the diffusion coefficient. In later developments, it was observed that this was attributable to the increased grain boundary area. From this fact it is learned that the diffusion coefficient in the grain boundary is much larger than that of the lattice. This would be imagined from previous discussions in this paper since the grain boundary has been pictured from a dislocation view point.

Early mathematical considerations pictured the grain boundary as a thin slab in which diffusion followed equation (3). This proved inadequate because the lattice has a finite diffusivity and because the grain boundary is physically very narrow. From these two facts, it is surmised that the concentration of material flowing down the grain boundary is partially lost to the lattice through diffusion.

Fisher (14) proposed an approximate solution to the diffusion equation considering this loss of material from the grain boundary. Fisher's model, as well as all subsequent models, treats the grain boundary as a very thin slab, of width δ which has a very high diffusivity and is surrounded by two semi-infinite slabs of low diffusivity material. Mathematically, he assumed that the diffusing material moves down the grain boundary, then flows out of it perpendicularly. This assumption is the result of experimental evidence that the grain boundary diffusivity is much larger than that of the lattice. From this assumption he derived a variation of Fick's second law which holds at $x = 0$ or in the grain boundary; diffusion proceeds in the y direction (independent of Z). This equation contains a term accounting for the loss of concentration to the lattice.

Within the grain boundary, at $x = 0$, constant diffusivity is assumed throughout the model,

$$\frac{\partial C}{\partial t} = D_b \frac{\partial^2 C}{\partial y^2} + \frac{2}{\delta} D_L \left[\frac{\partial C}{\partial x}\right]_{x=0} \qquad (7)$$

Outside the grain boundary, diffusion follows

$$\frac{\partial C}{\partial t} = D_L \nabla^2 C \; ; \qquad (8)$$

however, because he assumes that the diffusion is normal to the grain boundary, this equation reduces to

$$\frac{\partial C}{\partial t} = D_L \frac{\partial^2 C}{\partial x^2} \qquad (8a)$$

Equation (3) is a solution of equation (8a). Assuming an

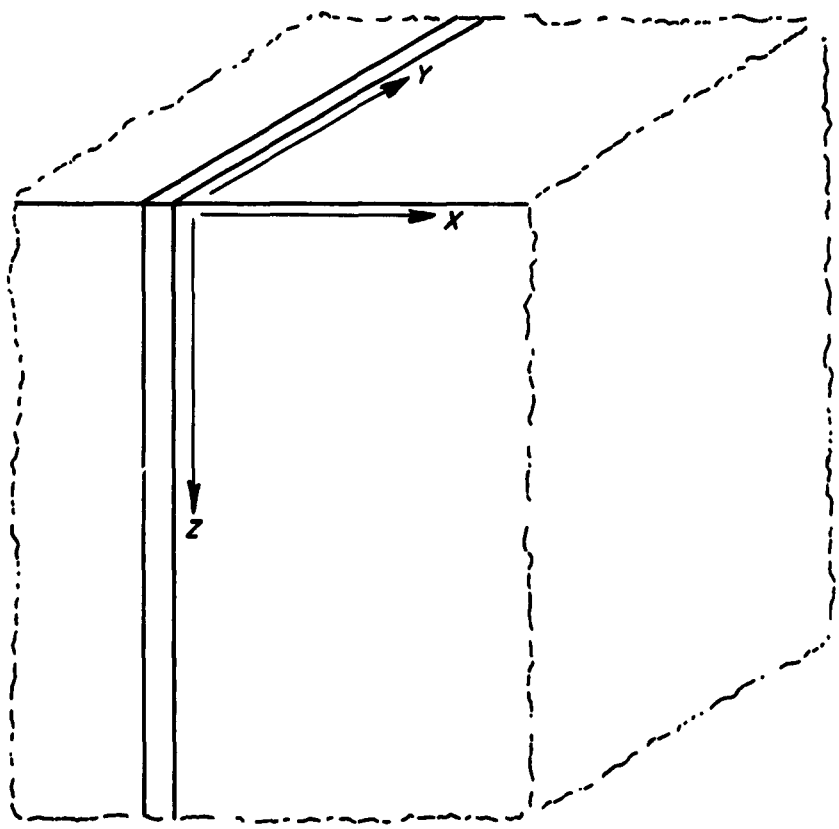

FIGURE 1. COORDINATE SYSTEM FOR GRAIN BOUNDARY DIFFUSION, ISOCONCENTRATION CURVES OCCUR IN THE X, Y PLANE.

infinite source and a product solution for the combined diffusion problem, equations 7 and 8,

$$C(x,y,t) = \varphi \left(1 - \text{erf}\left[\frac{x}{2\sqrt{(D_L t)}}\right]\right) . \qquad (9)$$

By applying equation (9) to (7) he solved the grain boundary diffusion problem; subject to the condition that φ from equation (9) follows the relation,

$$\frac{\partial \varphi}{\partial t} = 0 .$$

Fisher's solution is

$$C = C_o \left\{\exp\left[-\frac{4DL}{\pi t}^{\frac{1}{6}} \frac{y}{(\delta D_B)^{\frac{1}{2}}}\right]\right\} \left\{1 - \text{erf}\left[\frac{x}{2\sqrt{D_L T}}\right]\right\} \qquad (10)$$

Figure 2 shows a sample isoconcentration curve for Fisher's solution. As is noted, surface diffusion can be regarded as grain boundary diffusion in a quarter x, y plane bounded by a surface of thickness $\delta/2$. With surface diffusion, the diffusivity is larger than grain boundary diffusion as would be expected. Mechanistically this follows from an increased number of possible diffusion paths on the surface.

Whipple (45), being dissatisfied with Fisher's rash approximations, solved the same problem, but without the assumptions regarding time and diffusion direction. By using a Fourier-Laplace transformation, he was able to arrive at an exact solution with constant diffusivity and infinite source. The concentration is not expressible in elementary functions,

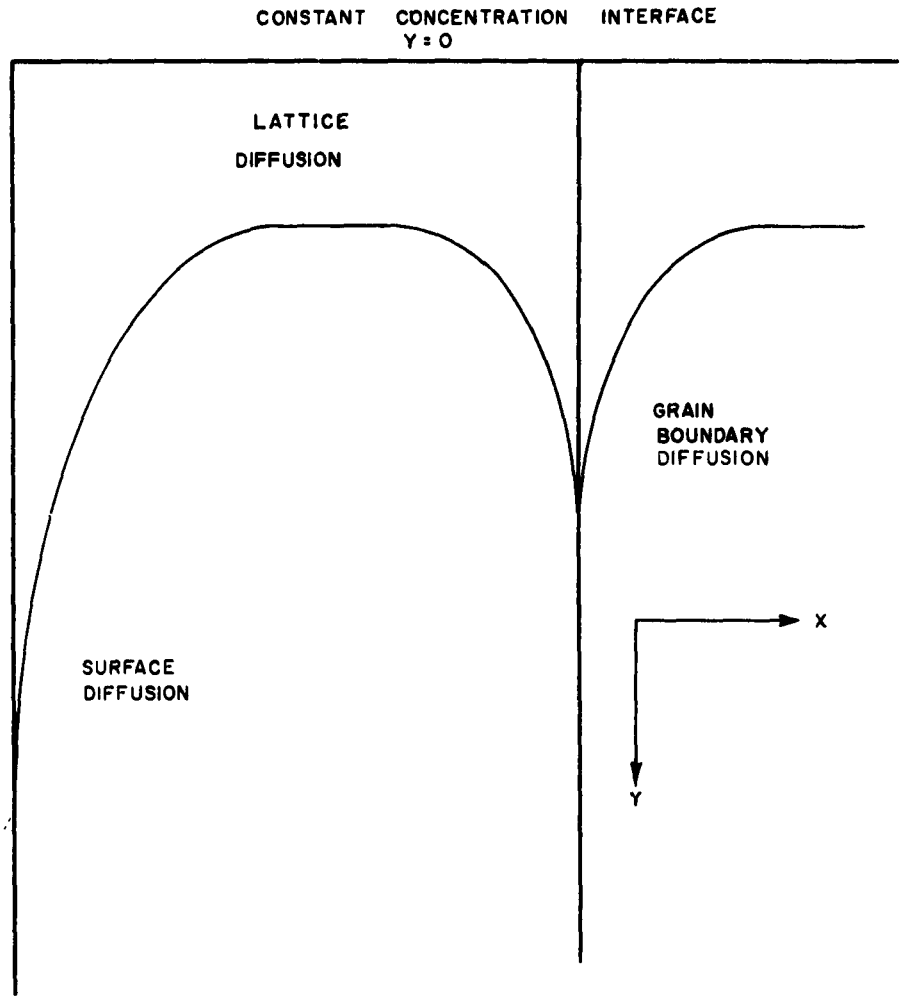

FIGURE 2. SAMPLE ISOCONCENTRATION CURVE DEMONSTRATING SURFACE AND GRAIN BOUNDARY DIFFUSION.

and it follows:

$$\frac{C}{C_o} = \operatorname{erfc} \frac{\eta}{2} + \frac{\eta}{2\sqrt{\pi}} \int_1^{\Delta} e^{-\eta^2/4\sigma} \operatorname{erfc} \left[\tfrac{1}{2} \left(\frac{\Delta - 1}{\Delta - \sigma} \right)^{\frac{1}{2}} \left(\frac{\sigma - 1}{\beta} + \xi \right) \right] \frac{d\sigma}{\sigma 3/2} \quad (11)$$

where $\eta = \frac{y}{(D_L t)^{\frac{1}{2}}}$, $\xi = \frac{x}{(D_B t)^{\frac{1}{2}}}$, $\Delta = \frac{D_B}{D_L}$,

and $\beta = \left[\frac{\delta}{2(D_L t)^{\frac{1}{2}}} (\Delta - 1) \right]$.

Equation (11) can not be expressed exactly in terms of elementary functions. In an attempt to overcome this, Whipple has approximated this function with an asymptotic series (i.e., the method of steepest descents).

$$\frac{C}{C_o} = 1.159 \, \beta^{1/3} \, \eta^{-2/3} \exp \left[-0.473 \, \beta^{-2/3} \, \eta^{4/3} + \beta^{-4/3} \, \eta^{2/3} \, (1 - \beta\xi) + \ldots \right] \quad (12)$$

A discussion of the relative validity of equations (10), (11), and (12) is to be presented later.

Borisov and Lyubov (8) developed equations based on Fisher's solution to cover the distribution of dissolved substance in polycrystalline grains and inter-crystalline boundaries. Their solution is subject to the same assumptions as Fisher's.

Grain boundary diffusion experiments are usually carried out by electroplating the substance to be diffused on the surface y = 0, see Figure 2. In most cases the amount of

substance deposited is too small to be considered an infinite source. For this reason, Suzuoka (39) resolved Whipple's problem utilizing a finite source. His boundary conditions are the same as Whipple's with the exception that $C(x,0,t) = C_o$ is replaced by $C(x,y,0) = KI(y)$, where $I(y)$ is defined by the relation

$$\int_{-\infty}^{\infty} f(y)\ I(y)\ dy = f(0)\ .$$

Utilizing a Fourier-Laplace transformation with the same variables as Whipple, Suzuoka found $C = C_1 + C_2$, where

$$C_1 = \frac{K}{\sqrt{\pi D_L t}} \exp \frac{-\eta}{4}\ , \text{ and}$$

$$C_2 = \frac{K}{\sqrt{\pi D_L t}} \frac{\partial^2}{\partial \eta^2} \left\{ \int_1^{\Delta} e^{-\eta^2/4\sigma}\ \operatorname{erfc} \left[\sqrt{\frac{\Delta - 1}{\Delta - \sigma}} \left(\frac{\xi}{2} + \frac{\sigma - 1}{\beta} \right) \right] \frac{d\sigma}{\sigma} \right\} . \tag{13}$$

Wood, Austin, and Milford (46) presented a discussion of the various grain boundary diffusion solutions. In their evaluation, they compared concentrations from Fisher's and Whipple's solutions. To solve the complicated equation (10) they used a Gaussian quadriture and a high speed computor. Their results show that the Fisher solution is valid only for short time intervals which are impractical in experimentation. Le Claire (29) in another analysis presented a graphical representation of the concentration values resulting

from the two theories. From this, one can arrive at an idea of the errors inherent in the Fisher approximation.

One of the incapabilities of these mathematical solutions must be discussed in view of the experimental results. Observing these equations (10), (11), (12) and (13), it is seen that one can not separate δ, the grain boundary width, with the data of a diffusion experiment. There have been attempts to find δ experimentally with little success. So, in any calculation of the grain boundary diffusivity, one must assume a δ to calculate D_b.

Four principal experimental methods have evolved to evaluate the validity of these mathematical models. The first is the so-called depth of penetration measurement. It consists of measuring the distance y at which a calibrated concentration appears in the grain boundary. The second is to find the tangent of the angle that an isoconcentration contour meets the grain boundary and to set the tangent equal to $[\partial(C/C_o)/\partial x] / [\partial(C/C_o)/\partial y]$. Third is the sectioning method where thin sections of the diffused specimen are analysed in comparison to $\int_o^y C/C_o \, dy$; this method analyses the amount of mass diffused. Fourth and final is the analysis of concentration by means of a microprobe analyser.

The simple tilt grain boundary has been viewed as stacked dislocations; in Figure 1 the dislocations would lie in the y direction. The dislocations are then separated by regions of high strain. With diffusion occuring in the dislocation direction, Turnbull and Hoffman (41) proposed that

the dislocation has a very high, constant diffusivity. The regions of strain between the dislocations have a diffusivity that is lower than that of the dislocation. The effective grain boundary diffusivity varies in the z direction (Figure 1), and as the distance between dislocations decreases, the grain boundary diffusivity increases. They experimentally determined a diffusivity for the dislocation pipe.

A change in the grain boundary angle does not alter the basic diffusion mechanism within a dislocation pipe; however, it does alter the boundary width or distance between dislocations. The activation energy for diffusion within any dislocation is only dependent upon the mechanism of diffusion within the pipe and is independent of the number of pipes if there were no energy interaction between successive dislocations. Therefore, if grain boundary diffusion occurs primarily within dislocation pipes, the activation energy change with misfit should result from the distance between dislocations.

Turnbull and Hoffman assumed the dislocation has a diameter ρ, and the distance between dislocations $d = a/[2 \sin(\theta/2)]$, where θ is the tilt angle and a is the lattice spacing. By treating the effective grain boundary width as

$$\delta(\theta) = \rho^2/d \qquad (14)$$

and using the grain boundary diffusion parameter $p = D_b\delta$, $p = D_b\rho^2 d$. However, due to equation (14), the boundary is

assumed, as far as diffusion is concerned, to be composed of dislocation pipes only. So,

$$p = D_p\delta = D_p\,\rho^2/d = 2D_p\,\sin(\theta/2)\,\rho^2/a\ . \qquad (15)$$

These theoreticians next pointed out that D_p should not be a function of θ. This is proven experimentally by solving for D_p in equation (15) from experimental conditions and the solutions of either Fisher or Whipple. The data used in their work comes from their analysis of the self-diffusion of silver-110 into silver tilt grain boundaries at five different temperatures for four different boundary angles between 9 and 28 degrees. It was noted that within experimental error, the calculated dislocation pipe diffusivity's activation energy was independent of tilt angle. The largest deviation in activation energy occurred at 28° tilt where they believe the dislocations interact.

Since grain boundary energy and migration are dependent on the angle of misfit, one would expect that the activation energy for grain boundary diffusion would also be. Flanagan and Smoluchowski (15), in studying the diffusion of silver into copper grains, observed that the activation energy for grain boundary diffusion decreased at small θ from the activation energy for lattice diffusion to a limiting value as θ increases. Similar work by Yukawa and Sinnott (47) also confirm this observation.

From Hoffman and Turnbull's work, one realizes that the activation energy for D_p is equal to the limiting value

for large angles of misfit in silver. This agreement between the activation energy for diffusion along the dislocation pipe, the diffusion at large angles of misfit, plus their predicted diffusivity behavior with misfit is a strong argument for the dislocation model grain boundary.

Upthegrove and Sinnott (42), in observing the activation energy for nickel self-diffusion in the grain boundary, found that it remains constant as θ changes between the angles 20° and 70°. Also, they noted that the ratio of grain boundary diffusivity to lattice diffusivity decreased from values of 10^7 at low temperatures to 10^4 at higher temperatures, causing a decreased penetration at the higher temperatures. This behavior is expected since the activation energy for grain boundary diffusion is much less than that of lattice diffusion; so, the ratio of the two would be expected to be temperature dependent.

Recalling again the work of Hoffman and Turnbull, their observations were made of diffusion down the dislocation pipes in a tilt boundary. The question arises as to whether the diffusivity would differ if diffusion were to take place perpendicular to the dislocation. Changes between the two were observed by Couling and Smoluchowski (11) and Achter and Smoluchowski (1). As expected, the largest difference is observed at low grain boundary angles. The reasoning behind penetration being larger when diffusion is down the dislocation pipes than in the other case is that diffusion parallel

to the pipes is carried primarily within the pipes. This point is carried in essence by Hoffman and Turnbull in that they assume that all diffusion in the grain boundary is within the dislocations. Diffusion perpendicular to these dislocations, in a very low angle boundary, would be almost entirely through the strained lattice between the dislocations. Extending this, one expects that as the dislocations move closer together (as in higher angle boundaries), the penetration parallel and perpendicular would become approximately the same. Couling and Smoluchowski (11) observe that there is no penetration difference in a 45° cubic tilt boundary.

Returning briefly to grain boundary energy, it is previously discussed that the energy of a grain boundary is concentration dependent. Phenomenologically, there was a difference in the strain energy when solute atoms are present. There should be some relationship between an increase in grain boundary strain energy and the amount of energy necessary to move an atom down the boundary. Since this strain field is altered by the presence of different types of atoms, it is expected that the energy for diffusion should also change with concentration. This type of grain boundary diffusion phenomena is studied by Austin and Richard (5) who analysed the diffusion of nickel into copper grain boundaries with a microprobe analyser. The grain boundary diffusivity was concentration dependent above 3 per cent nickel in a 45° tilt boundary and above 0.5 per cent in lower angles. This

dependence was noted as a deviation of isoconcentration curves from those predicted theoretically.

CHAPTER II

EXPERIMENTAL OBJECTIVES AND METHODS

The dependence of grain boundary energy on impurity content has been observed by several investigators. Grain boundary activation energy for self-diffusion should depend on the amount and type of impurity present. The investigation of this effect necessitates measurements of grain boundary self-diffusion in materials with varying impurity contents. To minimize experimental variables a constant grain boundary angular misfit is necessary. In a suitable boundary, segregation must occur. Due to the work of Thomas and Chalmers (40) the anglular misfit must be greater than 20° for sufficient segregation. The amount of segregation and its effect on the activation energy should depend on the type of impurity chosen; suitable choices for impurity types should attempt to show size and valence effects.

A coordinated study of angular and impurity effects in a single system is desirable. It would be impractical to study varying impurity contents over a wide range of boundary angles. The extrapolation of angle dependent activation energies to a higher angle at which impurity contents are varied would show any inconsistancies in the impurity data.

The commercial availability of lead with 99.9999 per cent purity has made possible an investigation of the type described above. This study has included grain boundary self-diffusion measurements in high purity lead with varying misfit angles. Impurity effects were studied for a single misfit angle, using different impurity species.

Grain boundary self-diffusion in the lead system was studied by radiography utilizing the low energy β emitting lead-210. This isotope possesses a long, 22 year, half life. Lead-210 primarily emits a 0.02 million electron volt β particle. This low energy β particle easily exposed the fine grain, thin emulsion used in contact autoradiography.

The major portion of the experimental program consisted of the following: crystal preparation and diffusion determinations.

Crystal Preparation

A modified Chalmers' (10) technique was used to provide seed crystals for bicrystal growth and bicrystals for diffusion specimens. This method is characterized by controlled solidification of molten metal in a suitable boat or container. Machinable refractory boats were constructed of aluminum silicate as shown in Figure 3 for single bicrystal growth. Since crystal growth is aided by having the boat at a higher temperature than the solidifying crystal, it was desirable to use boat material with a lower thermal conductivity than the lead charge. Thus heat flowed from the

boat into the crystal and proceeded out the chill block; this insured a wall temperature higher than the solidification front.

Bicrystals were grown in a manner similar to that of single crystals except two seed crystals were used. It was necessary for each seed to be oriented relative to one another to produce the necessary crystalline boundary. A special boat was constructed of lava to accomodate bicrystal growth. This boat differs from the single crystal boat in that two seed channels were necessary for bicrystals. Into each of these channels, an appropriately oriented crystalline seed of approximately 3 x 1 x 0.5 centimeters was placed. Bicrystals grown in this boat were approximately 1 centimeter high, 2 centimeters wide, and 15 centimeters long.

Clean high purity lead was placed as a charge in the boat; a seed crystal was placed in the channel at the open end. This assemblage was placed in a 28 millimeter pyrex tube which was sealed at both ends with appropriate modified Dresser pipe couplings. One coupling was connected to a chill block which came in contact with the crystal. The chill block was cooled by running water through it during crystal growth. Prior to growth the assemblage was flushed with nitrogen to reduce oxidation. A resistance heater, wound on a short length of vycor tubing which fitted externally concentric with the crystal boat, was used to melt the charge. Crystal growth then proceeded by melting the charge and the tip of the seed crystal and then slowly withdrawing the resistance

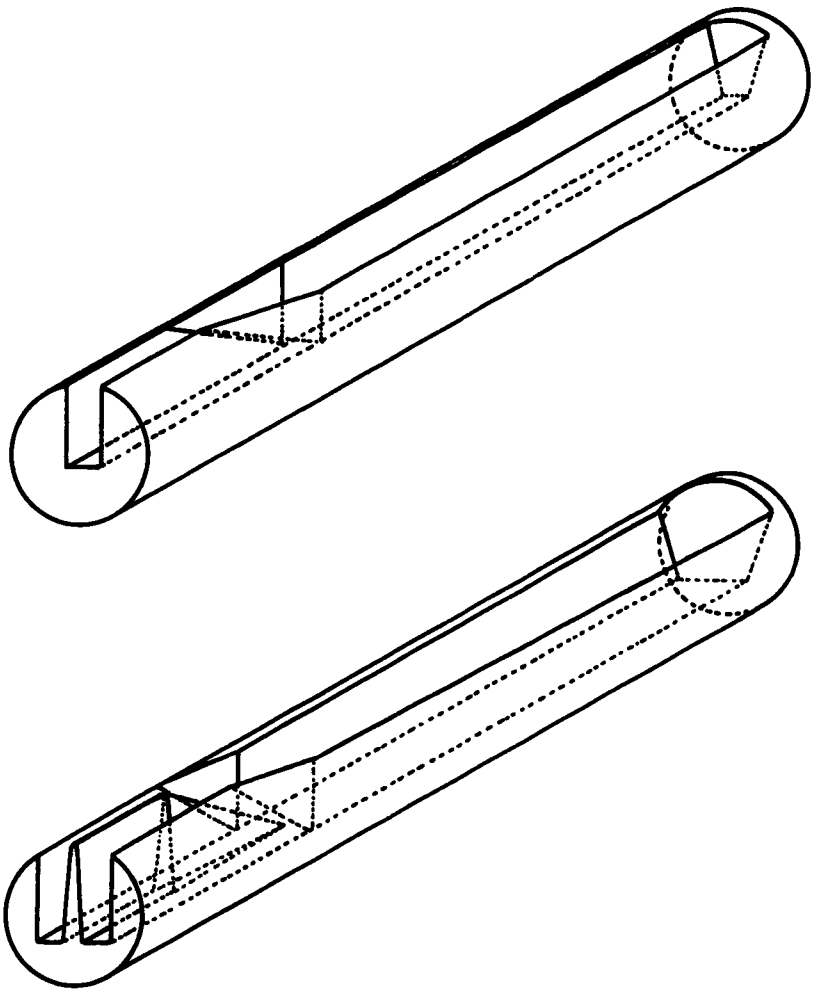

FIGURE 3. COMPARISON OF CRYSTAL GROWTH BOATS FOR SINGLE AND BICRYSTALS

heater from the molten charge at a rate of about three inches per hour. The growing crystal assumed the seed orientation. The orientation of these single crystals was verified by a back reflection Laue X-ray technique. Using the (100) easy growth direction in face centered cubic metals and aligning (001) planes parallel to the top surface, single crystals for subsequent bicrystal growth seeds were obtained. The seeds were cut to the desired orientation with a jeweler's saw.

Since high purity lead recrystallizes at room temperature, the abrasion of sectioning tended to recrystallize a thin layer of the crystal. This layer is removed by combined chemical-mechanical lapping with a solution. The lapping apparatus comprised a circular piece of Buehler A B Metcloth attached to plate glass; the cloth was saturated with a chemical polishing solution of one part glacial acetic acid and one part 30 per cent hydrogen peroxide. The disturbed crystal layer was removed by the combined chemical and mechanical action during a slow hand lapping.

Symmetrical tilt and twist grain boundaries were grown with the situations mentioned in Table I. These boundary angles were chosen as sufficient to determine the diffusion coefficient and activation energy dependence of misfit.

Solute elements for impurity dependent studies were chosen on the basis of atomic size and valence. One basic

TABLE I

CRYSTAL SPECIFICATIONS FOR THE STUDY OF ORIENTATION DEPENDENCE OF LEAD GRAIN BOUNDARY SELF-DIFFUSION

Material	Boundary	Misfit-degrees
99.999 + Pb	Symmetrical Tilt	θ = 3°,10°,14°,20°,30°
99.999 + Pb	Symmetrical Twist	θ = 4°,10°

consideration in impurity selection was solubility since it restricts the upper limit of impurity concentration. Reasonable solubilities in lead are demonstrated by bismuth, tin, indium, and thallium. Each of these elements represents a different type of impurity relationship in the lead system when atomic size, i.e., Goldschmidt diameter, and grouping in the periodic table are considered. Table 2 lists the solubility in lead, Goldschmidt diameter, and grouping of these for elements in the periodic table.

Alloys were made from lead with 99.9999 per cent purity. Measured amounts of these other elements of similar purity were added to the pure lead. Table 3 lists the alloy compositions used. Appropriate amounts of these elements and lead were melted under a nitrogen atmosphere; they were homogenized in the liquid state for a period of not less than four hours.

Tilt boundaries of thirty degrees of misfit were grown from these alloys. Thirty degrees was chosen as sufficient misfit for segregation. Since the angle of misfit is

TABLE 2

DESCRIPTION OF IMPURITY ELEMENTS

Material	Solubility in Lead Per Cent	Goldschmidt Diameter Å	Periodic Grouping
Pb	100	3.49	IV A
Bi	18	3.64	V A
Sn	1.9	3.16	IV A
In	50	3.14	III A
Tl	88	3.42	III A

TABLE 3

CONSTANT MISFIT ALLOYS FOR STUDY OF IMPURITY EFFECTS ON DIFFUSION

Material	Impurity Levels Wt. Per Cent
99.9999 % Pb with high purity tin additions	0%, 0.01%, 0.1%, 0.9%
99.9999 % Pb with high purity bismuth additions	0%, 0.1%, 0.7%, 1.5%
99.9999 % Pb with high purity thallium additions	0%, 0.05%, 0.3%, 1.5%
99.9999 % Pb with high purity indium additions	0.03%, 0.4%, 1.5%

constant in the impurity bicrystals, it was possible to grow the bicrystals within an impurity group (i.e. one type of alloying element) with a single bicrystal seed. The procedure consisted of preparing a bicrystal of pure lead with a thirty degree tilt between (010) planes. A bicrystal seed was then sectioned approximately one centimeter into the crystal from the point where the two seeds joined. After removing the recrystallized portion of the cut surfaces, the seed was used to prepare the lowest impurity bicrystal of one of the impurity groups. This procedure was repeated with the next highest impurity concentration in the same group. This method of reusing a bicrystal seed was employed to produce the necessary bicrystals. It was necessary to provide an original bicrystal seed for each group to prevent intercontamination between the groups. For the 30° tilt boundary the misfit was reproducible to within ±1° in an impurity group and to within ±3° between the impurity groups.

Diffusion Determinations

The determination of the diffusion profile resulting from grain boundary penetration was based on radioactive tracer measurements using a method of high resolution autoradiography described by Gomberg *et al* (19). The method used a permeable base autoradiographic stripping film, Eastman Kodak Permeable Base Autoradiographic Stripping Film. This film is used in direct contact with the diffusion profile as is to be described. Radioactive lead-210 was

purchased as a nitrate in nitric acid solution from Atomic Energy of Canada, Commercial Products Division.

The radioactive lead was received as a nitrate in nitric acid solution and was converted to an electroplating solution of inert lead and radioactive lead-210 in the chemical form of lead fluoroborate. Lead carbonate was precipitated from the nitrate solution by adding sodium carbonate, as described by Gray (21). Fluoroboric acid was produced by reacting boric acid with hydrofluoric. The resulting acid, when added to lead carbonate, forms lead fluoroborate and evolves carbon dioxide. The lead-210 nitrate was received with an activity of 2.5 millicuries per milligram. This was diluted to approximately 1 millicurie per gram with inert lead. This dilution permitted reasonable handling safety and exposure periods. Further dilution would have merely increased the amount of time necessary for a good autoradiographic exposure.

The bicrystals were sectioned in lengths of 1.5 centimeters with the surface to be plated perpendicular to the grain boundary dislocation pipes. This surface was etched with a solution of 2 parts glacial acetic acid, 1 part 30 per cent hydrogen peroxide, and 1 part water. All of the surface except the portion of the grain boundary was masked off. The mask consisted of a square inch of electrical tape with a hole approximately 5/32 inch in diameter which covered the area to be plated. This area was polished with the

previously described lapping solution under an inert atmosphere in a dry box. After drying the area with a stream of nitrogen, a drop of active plating solution (about 0.04 milliliters) was placed directly on the crystal. The drop was depleted of lead after about six minutes of electroplating at 2 milliamperes. This produced an active layer about 40 microns in thickness; this thickness was presumed to be sufficient to keep a constant concentration at the surface during diffusion.

The primary reason for plating in this unusual manner was the adverse results obtained when a plating cell was used. Early attempts to use a cell which contained the active plating solution resulted in a small amount of recrystallization where the cell contacted the specimen. At the high temperatures used in the diffusion anneals, this recrystallized area suffered grain growth destroying the crystal.

Following plating of the radioactive isotope, the crystals were put in a diffusion cell shown in Figure 4. The cell was constructed of a long pyrex tube sealed with a modified Dresser pipe coupling. Inside the cell were pyrex cups containing pyrex wool filtering fiber. The diffusion specimens rested on the pyrex wool. When the cell was full of specimens it was flushed several times with argon. This static inert atmosphere kept the specimens from oxidizing during the diffusion anneal. Subsequent to the argon flushing, the cell full of specimens was placed in an isothermal bath for the diffusion annealing treatment.

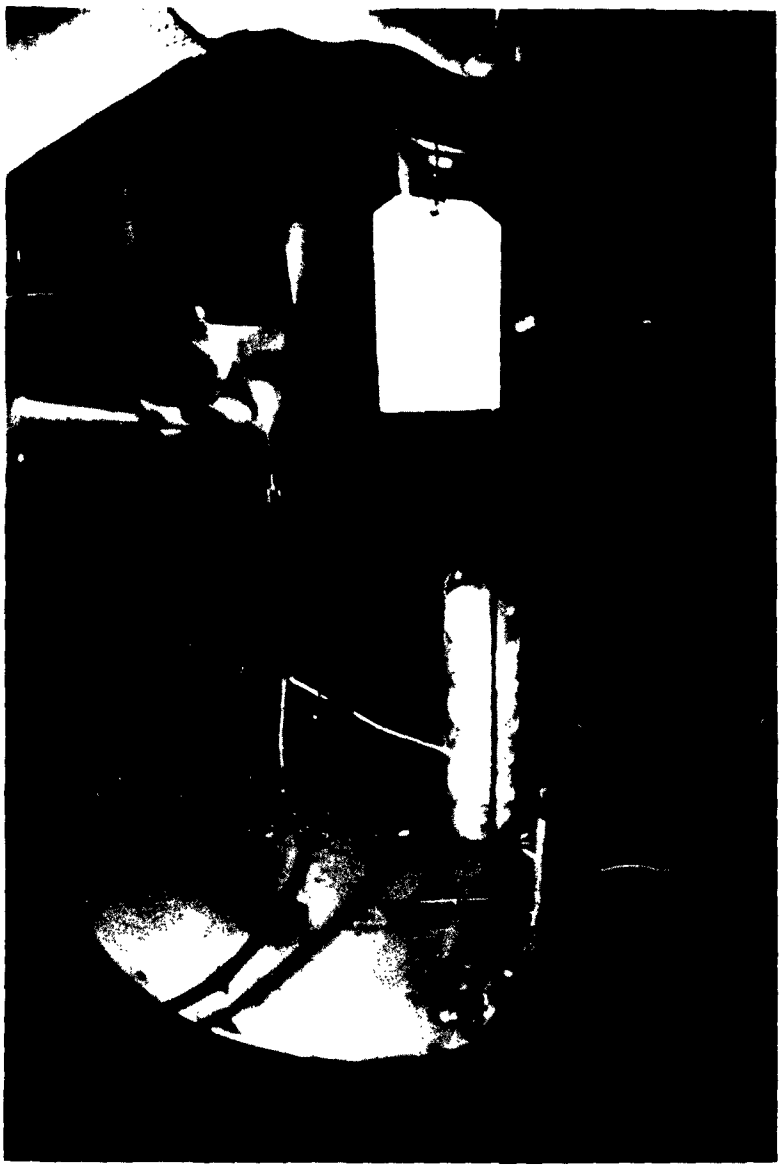

Figure 4. The Diffusion Cell and Isothermal Bath Used to Anneal Diffusion Specimens

Theoretically, two temperatures should be sufficient to determine D_o and Q from equation 3. From a practical standpoint, however, four different temperatures between 120° and 220°C were selected with their appropriate diffusion times (see Table 4). Results obtained from these tests were analysed statistically to obtain the best least-square fit of the Arrhenius equation. As mentioned in the introduction, there are four methods for determining values for the diffusion coefficient. The ease and inherent accuracy of contact autoradiography dictated a depth of penetration measurement. In this procedure, the distance y along the grain boundary at which a known concentration appeared was measured. Knowing the lattice diffusion coefficient and the time, a value for the D in the grain boundary was determined.

TABLE 4

DIFFUSION TEMPERATURES AND THEIR RESPECTIVE TIMES USED IN LEAD GRAIN BOUNDARY SELF-DIFFUSION ANALYSES

Temperature °C	Time Days
120	8
143	7
166	5
220	4

The original Gomberg (19) technique consisted of applying the stripping film to a mounted specimen which was

sectioned and polished in the standard manner. Then, following an exposure, the film could be chemically processed and the measurements would be made directly on the specimen without disturbing the film. The specimen is kept clean by a thin organic coating impermeable to the processing chemicals. This coating protects the polished metal surface so that the radiographic density is directly observable.

A combination of two factors prevented the use of this procedure in this research. First, lead is mechanically too soft for ordinary polishing techniques and the lapping procedure was necessary. It was impossible with this technique to maintain the required edge preservation with a plastic mounted specimen. Second, that film processing chemicals actively attacked the polished surface and no impermeable coating could be found to stop this.

This chemical attack necessitated the development of a method to remove the film from the specimen for processing and examination. The method of autoradiography used consisted of protecting the specimens with an additional layer of lead. This was done by electroplating each specimen with inert lead to a depth of about one millimeter. This overplate protected the edge of the specimen which would normally be rounded by the chemical lapping procedure. Following the overplating, the specimens were sectioned perpendicular to the active button and grain boundary yielding a surface parallel to the diffusion direction. This surface was then polished flat by the previously described chemical-mechanical procedure.

The autoradiographic stripping film was removed from its backing and floated on water. The floating procedure was necessary since the emulsion and its gelatin backing expand in water, and dimensional changes could not be tolerated subsequent to the exposure. When full expansion had taken place the film was mounted on a 7/8 inch square glass cover slide with the gelatin side down, see Figure 5. Any bubbles between the film and slide were removed with filter paper. The film and slides were then dried in air. Since the film is rather insensitive to light, this proceedure, as well as subsequent ones, could be performed under the red light of a Kodak Wratten Series #2 Filter.

Film and specimen holders were fashioned from rubber hose clamps by glueing rubber pieces to the clamp faces. Exposures were then made by placing the film side of the glass slide in contact with the polished crystal surface and mounting them in the clamps. Figure 6 demonstrates the mounting procedure for the exposure runs. The relatively high activity of the radioactive plate made exposures of 2.5 hours sufficient. After the exposures, the slides were removed from the clamps and inserted in artery clamps for ease of handling during chemical processing.

Chemical film processing involved developing in Kodak D-19 developer diluted 1 part stock solution and 2 parts water for 90 seconds, stopping with water, and fixing in Kodak Fixer for 10 minutes. Final washing time was 15 minutes

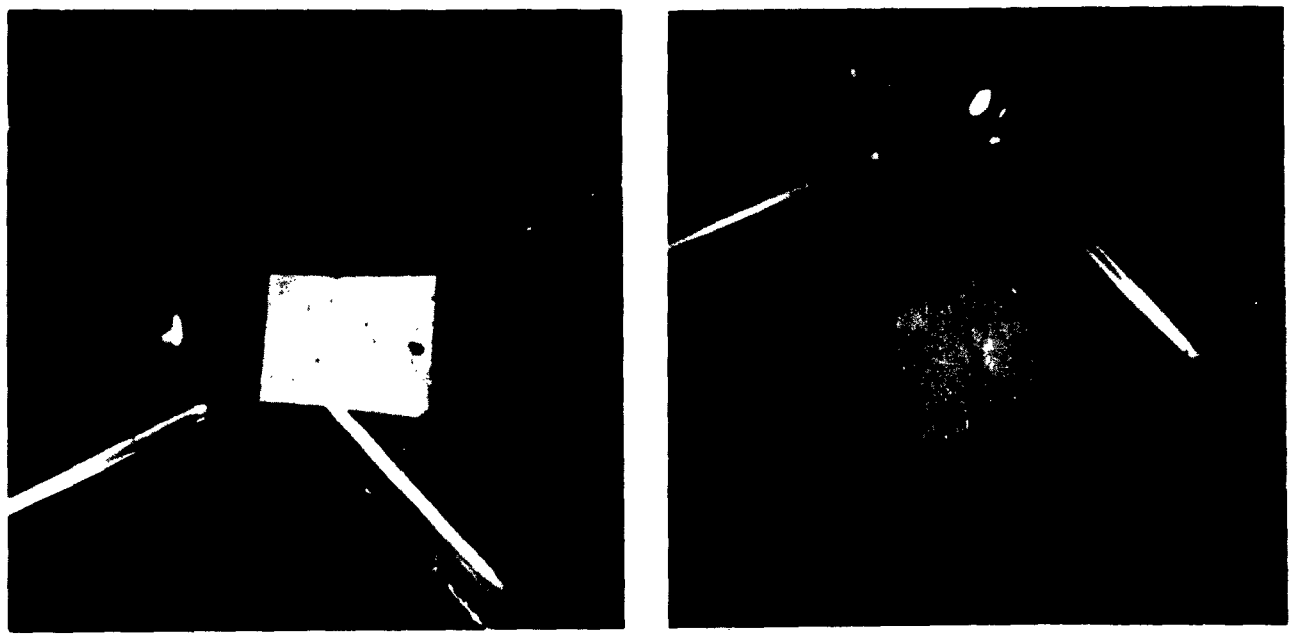

Figure 5. Representation of the Technique of Mounting Photographic Emulsion on Glass Cover Slides

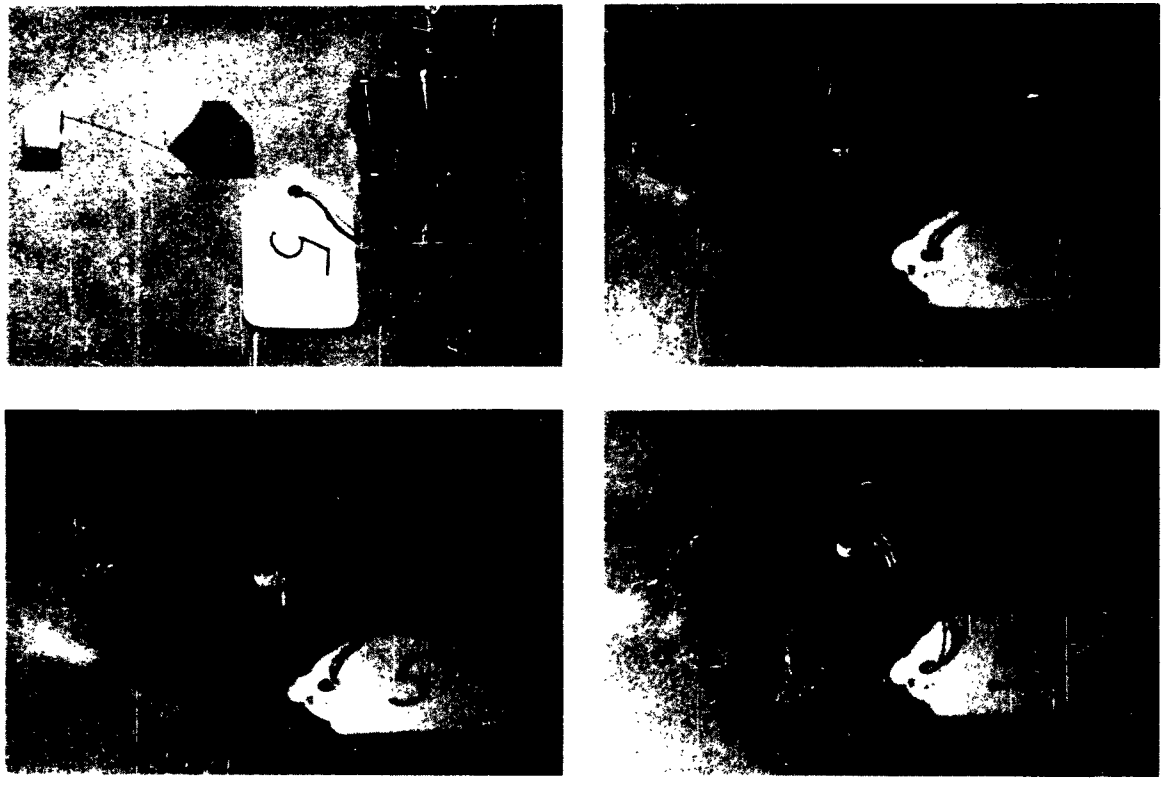

Figure 6. Method of Clamping Film to Diffused Specimen for Autoradiographic Exposure

followed by drying in air. Subsequent to drying, the fine grained film is analysed by photomicrography while still attached to the cover slide.

Calibration was necessary to determine the concentration at the depth of boundary penetration y. This concentration is determined by making some autoradiographic standards. These autoradiographic standards were homogeneous alloys of active lead in inert lead with varying specific activity. Preparation was accomplished by plating an inert lead chunk weighing about 15 grams with active lead. These were then homogenized for 12 hours in an inert atmosphere 60 degrees above the melting point of lead. The percentage of active lead to inert lead is as follows:

$0.0\%\ Pb^{210}$

$9.96 \times 10^{-4}\%\ Pb^{210}$

$4.68 \times 10^{-3}\%\ Pb^{210}$

$9.32 \times 10^{-3}\%\ Pb^{210}$.

Autoradiographs of these four samples were then taken in exactly the same manner as the diffusion specimens.

CHAPTER III

EXPERIMENTAL RESULTS

The experimental method in this work involved diffusing a specimen for a time and measuring the grain boundary penetration distance to a determined concentration C/C_o. The desired concentration ratio selected was determined by autoradiography and was the minimum concentration ratio observable above background, that is, autoradiographs are compared to 0.0 per cent active lead. The motion of β particles through the emulsion, darkens it upon processing. The density of the autoradiograph then consists of the number of exposed emulsion grains per unit area. It is impossible to obtain a perfectly clean autoradiograph, even with no exposure to radioactivity. This is due to a certain amount of dirt accumulating on the autoradiograph. In addition, phenomena such as pressure sensitive development, cosmic radiation, and self activation cause film background. During the polishing the active specimens, some active atoms will accumulate on the specimen surface where no activity should be observed. These two types of contaminates comprise the background density observed on the autoradiograph. The calibration concentration used was the minimum concentration

observable above background. This concentration was used because it lies at the maximum distance from the plated interface, and, as will be shown later, an increase in the penetration distance measured increases the experimental accuracy.

The background concentration was determined at the same time and in the same manner as the calibration concentrations. Polishing procedures for all active specimens had to be constrained to a restricted enclosure for safety reasons, therefore, the calibration specimens suffered some intercontamination. Of the calibration specimens used, the background concentration most closely resembled 9.96×10^{-4} per cent; however, there was little difference between 9.96×10^{-4} per cent and 4.68×10^{-3} per cent. From this the cutoff concentration was judged to be $C/C_o = 10^{-5}$.

Penetration measurements of grain boundary diffusion were divided into three different areas of interest. The penetration values were obtained by enlarging the processed autoradiograph fifty times on a metallograph and measuring the penetration. The areas of interest involve variations in grain boundary misfit, impurity content, and a check on the validity of Fisher's mathematical solution by varying the time at constant temperature and boundary angle. The diffusion temperatures and their respective times for impurity and misfit studies are given in Table 4.

Recalling equation (9), Fisher's solution predicts that the penetration y should vary with $t^{\frac{1}{4}}$. Investigators

such as Upthegrove and Sinnott (44) show that this dependence is true only for extremely large angle grain boundaries. For this reason, a test of the validity of Fisher's solution in lead was obtained by determining penetration values with constant misfit and temperature for varying times. This has been done for some 20° and 30° tilt boundaries of pure lead at 220°C. The highest temperature was chosen because it represents a test of the model under the most adverse experimental conditions in this investigation. That this is the case follows from Fisher's assumption that lateral diffusion out of the grain boundary proceeds perpendicular to it. This may be concluded from his assumption that D_b is so much larger than D_L that diffusion follows the grain boundary, then proceeds normal to it. Lattice and grain boundary diffusion have different activation energies; D_b/D_L is smaller at higher temperatures than at lower ones. Since the diffusion direction is perpendicular to an isoconcentration contour, one expects that Fisher's assumption about the diffusion direction being normal to the grain boundary is only strictly true for D_b/D_L equals infinity, therefore, the selection of conditions under which D_b/D_L is minimum provided the most severe test of Fisher's model.

The dependence of the magnitude of D_b/D_L and the resultant change in the shape of the isoconcentration interface and diffusion direction can be seen from the autoradiographs of Figure 7.

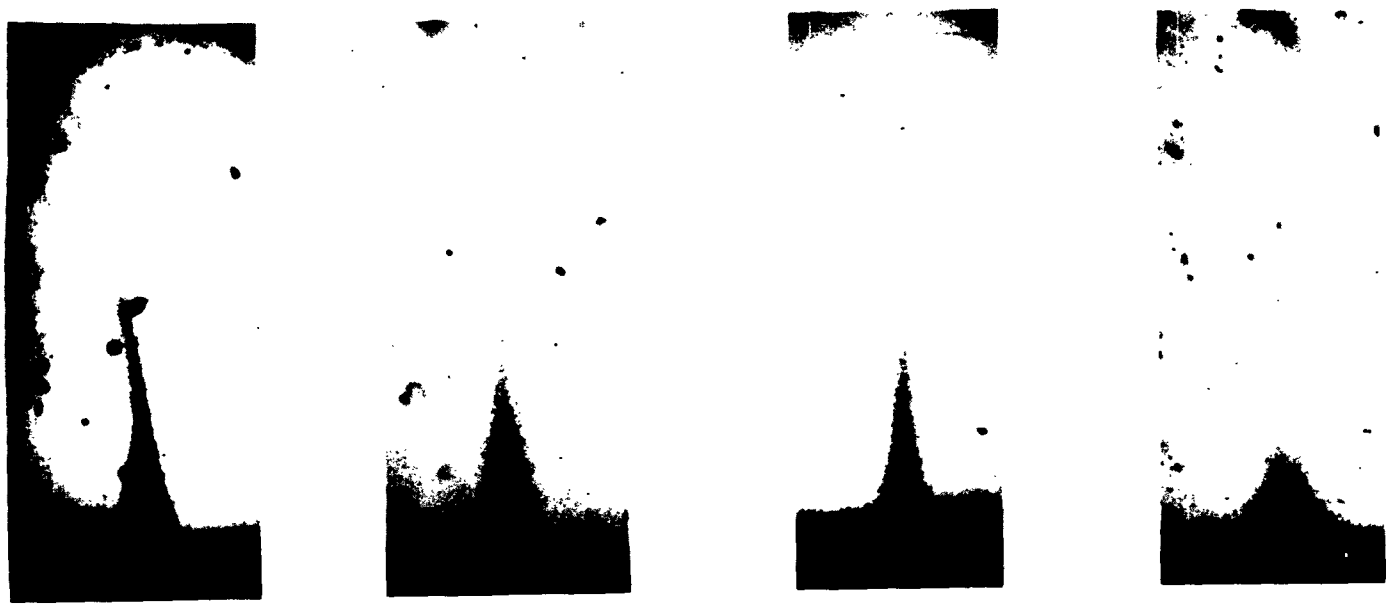

T = 120° C T = 143° C T = 166° C T = 220° C

Figure 7. Autoradiographs of 30° Tilt Angle Specimens Diffused at Different Temperatures Demonstrating Differences in Isoconcentration Profiles

In these photographs it can be seen that the isoconcentration contours at low diffusion temperatures are long and thin. This is expected when D_b/D_L is very large. The change in D_b/D_L with temperature can be seen from the angle with which an isoconcentration contour meets the boundary.

Table 5 presents observed penetrations for varying time at 220° C.

TABLE 5

TIME DEPENDENCE OF LEAD - 210 PENETRATION INTO 30° LEAD TILT BOUNDARIES, A VALIDITY TEST FOR FISHER'S SOLUTION

Time Sec.	Misfit Degrees	Penetration cm.
8.64×10^4	30°	0.042
8.64×10^4	30°	0.040
8.64×10^4	30°	0.040
8.64×10^4	30°	0.042
1.73×10^5	30°	0.042
1.73×10^5	30°	0.044
6.92×10^5	30°	0.066
6.92×10^5	30°	0.068

Experimental observations of penetration as a function of time, misfit and temperature are presented in Table 6.

Table 7 shows the penetration results observed for diffusion in 30° bicrystals of lead in which the impurity concentration was varied as shown. The experimental conditions of time and temperature were the same as those for misfit dependence.

TABLE 6

PENETRATION, TIME, AND TEMPERATURE OBSERVATIONS OF THE MISFIT DEPENDENCE OF LEAD GRAIN BOUNDARY SELF-DIFFUSION

Angle Degrees	Penetration cm.	Time ($x10^{-5}$) Sec.	Temperature °C
3° Tilt	0.044	6.92	120
	0.030	6.05	143
4° Twist	0.040	6.92	120
10° Tilt	0.002	6.92	120
	0.025	4.32	166
	0.012	3.46	220
10° Twist	0.025	6.92	120
	0.028	6.05	143
	0.028	4.32	166
	0.012	3.46	220
14° Tilt	0.041	6.92	120
	0.048	6.05	143
	0.030	4.32	166
	0.016	3.46	220
20° Tilt	0.118	6.92	120
	0.086	6.05	143
	0.058	4.32	166
	0.034	3.46	220

TABLE 7

PENETRATION, TIME, AND TEMPERATURE DEPENDENCE OF LEAD GRAIN BOUNDARY SELF-DIFFUSION WITH VARYING IMPURITY CONTENTS IN 30° TILT BOUNDARIES

Impurity Level per cent	Penetration cm.	Time ($\times 10^{-5}$) Sec.	Temperature °C
0% Tl	0.176	6.92	120
	0.134	6.05	143
	0.105	4.32	166
	0.062	3.46	220
0.05% Tl	0.166	6.92	120
	0.134	6.05	143
	0.095	4.32	166
	0.056	3.46	220
0.3% Tl	0.172	6.92	120
	0.138	6.05	143
	0.108	4.32	166
	0.054	3.46	220
1.5% Tl	0.152	6.92	120
	0.118	6.05	143
	0.072	4.32	166
	0.048	3.46	220
0.03% In	0.100	4.32	166
	0.066	3.46	220
0.4% In	0.066	3.46	220
1.5% In	0.132	6.92	120
	0.070	4.32	166
	0.041	3.46	220
0% Sn	0.160	6.92	120
	0.132	6.05	143
	0.093	4.32	166
	0.056	3.46	220
0.01% Sn	0.166	6.92	120
	0.136	6.05	143
	0.085	4.32	166
	0.054	3.46	220

TABLE 7--Continued

Impurity Level per cent	Penetration cm.	Time (x 10^{-5}) Sec.	Temperature °C
0.1% Sn	0.162	6.92	120
	0.134	6.05	143
	0.088	4.32	166
0.9% Sn	0.144	6.92	120
	0.092	6.05	143
	0.065	4.32	166
	0.046	3.46	220

CHAPTER IV

DATA ANALYSIS

In the determination of the diffusion coefficients in the grain boundary, the mathematical solutions of the diffusion equation are applied to the experimental results. Additional information was needed in both Whipple's and Fisher's solutions because both theories require information on the lattice diffusion coefficient at the temperature of the measurement. Also, for an exact solution of grain boundary diffusivities, information is needed on the width of the grain boundary during the diffusion measurement. However, activation energies for grain boundary diffusion can be obtained from Fisher's solution without knowledge of the grain boundary width by plotting $D_b\delta$ vs. $1/T$ on semilogarithmic paper, and measuring the resulting slope. As will be discussed, this is true to a good approximation in Whipple's solution when the penetration is observed within the grain boundary ($x = 0$).

Data evaluation, in terms of boundary diffusivities from either the Whipple or Fisher solution, requires knowledge of lattice diffusion coefficients at the temperature in question. Lattice diffusion can be measured at the same time as grain boundary diffusion; however, because of the

errors involved in this measurement, the results of lead self-diffusion by Hudson et al. (27) were used. These self-diffusion coefficients were obtained by taking the least-square fit to the Arrhenius equation, under their experimental conditions, and extrapolating to the temperatures used in this investigation.

In evaluation of the impurity bicrystal diffusion coefficients, it was necessary to assume that the values for pure lead lattice diffusion were sufficiently accurate. This assumes that the lattice diffusion coefficients were independent of the impurities used. The validity of this assumption is supported by the experimental results of Resing and Nachtrieb (37) who have studied lead self-diffusion with varying thallium additions. Their work engulfed the whole spectrum of possible concentrations of thallium in lead; an example of their results (Table 8) shows activation energy changes with thallium content. From the small changes in activation energy and an observed 10 per cent variation in lattice diffusivities between 0 per cent and a 20 per cent Tl, it is reasonably assumed that almost no change would follow in bismuth, tin, and indium for the concentrations less than 1.5 per cent by weight. Table 9 shows the lattice diffusion coefficients used in this investigation.

Preliminary efforts to solve Whipple's equation (11) for the experimental conditions of this investigation were unsuccessful. A Gaussian quadrature solution of the thirty

TABLE 8

ACTIVATION ENERGY FOR LEAD LATTICE SELF-DIFFUSION WITH VARYING THALLIUM CONCENTRATIONS (37)

Activation Energy Kcal/gm.mole	Thallium Content per cent
26.1	0
25.5	10
25.0	20
24.8	30
24.5	40

TABLE 9

LEAD LATTICE SELF-DIFFUSION COEFFICIENTS USED IN GRAIN BOUNDARY MATHEMATICAL SOLUTIONS WITH THEIR RESPECTIVE TEMPERATURES (26)

Diffusivity $cm.^2/sec.$	Temperature °C
1.18×10^{-14}	120
6.82×10^{-14}	143
3.28×10^{-12}	166
7.17×10^{-12}	220

second order was insufficient. However, in certain data cases, the requirements of equation (12) were met.

$$\frac{C}{C_o} = 1.159\ \beta^{1/3}\ \eta^{-2/3} \exp\left[-0.473\ \beta^{-2/3}\ \eta^{4/3} + \beta^{-4/3}\ \eta^{2/3}\ (1 - \beta\xi) + \ldots\right] \tag{12}$$

The data of this investigation apply in the grain boundary where $\xi = 0$. When $\xi = 0$, C/C_o is only a function of η and β. The grain boundary diffusivity and width both appear in β, but not in η.

$$\beta = \delta(\Delta - 1) \,/\, 2(D_L t)^{\frac{1}{2}}$$

$$= \left[\delta/2(D_L t)^{\frac{1}{2}}\right] (D_b/D_L - 1)$$

$$\approx \left[\tfrac{1}{2}(D_L t)^{\frac{1}{2}}\right] (\delta D_b/D_L) \ .$$

In this investigation $D_b/D_L > 10^3$; so $D_b/D_L >> 1$. To a good approximation C/C_o is a function of $D_b\delta$ as in Fisher's solution. Since Fisher's model, equation (10), and Whipple's model, equation (12), both involve the product $D_b\delta$, an arbitrary choice of δ for all diffusion situations will not affect the activation energy. This comes from the fact that $D_b\delta$, the diffusion parameter, is a function of temperature by the Arrhenius equation; however, δ is assumed a constant 10^{-7} centimeters in this investigation. Tables 10 and 11 give comparative grain boundary diffusivities ($\delta = 10^{-7}$ centimeters) for both the Whipple and Fisher equations. A sample calculation of diffusivity using Fisher's equation is given in Appendix C.

TABLE 10

MISFIT DEPENDENCE OF LEAD GRAIN BOUNDARY SELF-DIFFUSION COEFFICIENTS AS ANALYSED BY THE FISHER AND WHIPPLE SOLUTIONS

Angle Degrees	Temperature °C	Diffusivity $cm^2/sec. \times 10^7$ Fisher	Whipple
3° Tilt	120	0.213	0.515
	143	0.256	0.612
4° Twist	120	0.176	0.425
10° Tilt	120	0.053	0.127
	166	0.462	1.09
	220	0.554	
10° Twist	120	0.069	0.165
	143	0.224	0.538
	166	0.573	1.37
	220	0.554	
14° Tilt	120	0.181	0.439
	143	0.656	1.56
	166	0.661	1.60
	220	0.986	
20° Tilt	120	1.53	3.08
	143	2.10	5.06
	166	2.47	5.93
	220	4.59	

TABLE 11

IMPURITY DEPENDENCE OF LEAD GRAIN BOUNDARY SELF-DIFFUSION COEFFICIENTS AS ANALYSED BY THE FISHER AND WHIPPLE SOLUTIONS

Impurity Level per cent	Temperature °C	Diffusivity $cm^2/sec. \times 10^7$ Fisher	Whipple
0% Tl	120	3.40	8.20
	143	5.11	
	166	8.07	19.5
	220	14.8	34.9
0.05% Tl	120	3.03	7.31
	143	5.11	
	166	6.61	16.0
	220	12.1	28.5
0.3% Tl	120	3.25	7.85
	143	5.40	
	166	8.59	20.7
	220	11.2	26.4
1.5% Tl	120	2.54	6.10
	143	3.95	
	166	3.82	9.16
	220	8.86	20.71
0.03% In	166	7.34	17.8
	220	16.7	39.8
0.4% In	220	16.7	39.8
1.5% In	120	1.91	4.63
	166	3.60	8.62
	220	6.47	14.9
0% Sn	120	2.82	6.75
	143	4.94	11.9
	166	6.35	15.3
	220	12.1	28.5
0.01% Sn	120	3.03	7.32
	143	5.25	12.5
	166	5.30	12.7
	220	11.2	26.4

TABLE 11--Continued

Impurity Level per cent	Temperature °C	Diffusivity $cm^2/sec. \times 10^7$ Fisher	Whipple
0.1% Sn	120	2.88	6.96
	143	5.11	12.3
	166	5.68	13.7
0.9% Sn	120	2.28	5.49
	143	2.40	5.74
	166	3.1	7.45
	220	8.16	19.0

The precision and accuracy of the diffusion coefficients in the grain boundary are dependent on the validity of the constant lattice diffusivity assumption, the assumption of the value of δ, and the measurements of time and penetration. Diffusion times were at least one day, and if it were assumed that a total of ten minutes elapsed in heating and cooling the specimens, then the error in time would be much less than 1 per cent. Errors in depth of penetration measurements yield diffusion coefficient uncertainties much larger than this.

The method of obtaining penetration values was subject to error. Sources of accumulation occur in the removal of the film from the specimen for processing and in the inherent resolution of the film technique. Because the film was removed from the specimen for processing, measurements made upon it required an estimation of the position of the

constant concentration interface. Lattice diffusion is small, because of the low temperatures used; therefore, the interface position was estimated as the edge of lattice diffusion. An appropriate correction of 0.002 centimeters was introduced at 220° C to account for the lattice diffusion penetration. The polished surface of the specimen is not precisely flat, thus, there is a possibility of β particles leaving the diffused area at an acute angle to the specimen surface and thereby spreading the autoradiograph. When this spreading appeared to be sufficient to impair greatly the results, the specimen was repolished, and another autoradiograph taken. The composite penetration uncertainty from these means was roughly estimated from the results of the time dependence study since several crystals were diffused under the same conditions. Comparing penetration values from Table 5, the estimated error of ± 0.003 centimeters is expected. This estimated error + 0.003 centimeters would yield diffusion coefficient errors; calculations for a 30° tilt boundary in pure lead are given in Table 12. As is noted in the table, diffusion coefficients of the 30° boundaries should be reliable to within 11 per cent. The error in diffusion coefficients associated with this error in penetration would be larger in low angle boundaries and high temperature diffusion runs because of the smaller absolute penetrations involved. The expected increase in this deviation is consistent with the greater data scatter shown in Figure 8. The activation

energy for grain boundary diffusion is obtained by the method of least squares fit in order to minimize the influence of data scatter on the activation energy and frequency factor.

TABLE 12

DEVIATION OF LEAD GRAIN BOUNDARY DIFFUSIVITY OF A 30° TILT BOUNDARY DUE TO PENETRATION MEASUREMENT ERROR OF +0.003 CENTIMETERS*

Diffusivity Fisher's Solution $cm^2/sec.$	Error Per cent	Temperature °C
$3.40 \pm 0.12 \times 10^{-7}$	10.7%	120
$5.11 \pm 0.22 \times 10^{-7}$	10.4%	143
$1.48 \pm 0.10 \times 10^{-6}$	10.7%	220

*$\delta = 10^{-7}$ cm. used

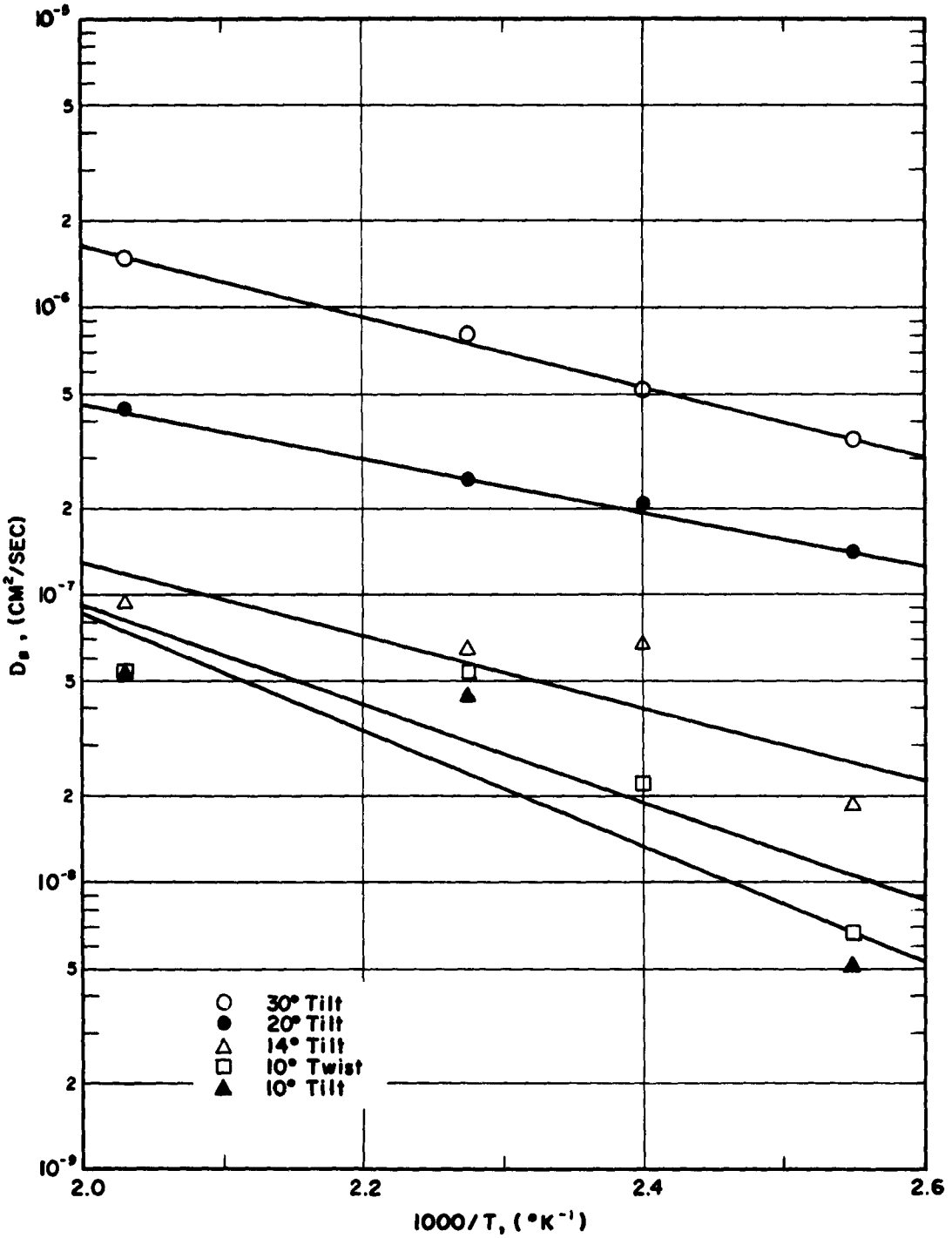

FIGURE 8. TEMPERATURE AND MISFIT ANGLE DEPENDENCE OF THE LEAD GRAIN BOUNDARY SELF-DIFFUSION COEFFICIENT, DATA ANALYSED FROM FISHER'S ANALYSIS

CHAPTER V

DISCUSSION OF RESULTS

Bicrystals used in this study were grown from the melt in the manner described. Inherent in these bicrystals was a certain amount of imperfection such as is characteristic of crystals grown from the molten state. These imperfections took two forms: subgrains and stray grains nucleated during growth. These two occurrences plagued this research through its entirety.

There was no exact correlation in the frequency with which these imperfection types occurred for the few crystals grown; however, there appeared to be a relation between the occurrence of these imperfections and the bulk impurity content. This observation is based on the number of times it was necessary to regrow bicrystals and the degree of perfection of the resulting crystal. It appeared that both very high purity and low purity crystals were extremely difficult to grow. In general there was no difficulty in growing crystals in the range of 99.9 to 99.99 per cent purity for any of the alloying elements: tin, indium, bismuth, or thallium. Crystals of higher purity than 99.99 per cent exhibited

supercooled liquid. Non-equilibrium inhomogeneous composition can occur between this supercooled liquid and the solidified metal resulting from composition fluctuations. The inhomogeneous composition can then nucleate stray grains.

The phenomena of grain boundary diffusion, energy and migration have been discussed relative to changes in boundary misfit. High grain boundary angles can usually be considered as a transition region between crystalline order and liquid disorder. This is attributable to the increase of porosity with misfit. Diffusion data obtained for varying misfit supports this supposition, Table 10; the grain boundary diffusion coefficient increased with the angle of misfit. This dependence is not unique in the lead system and has been observed in many repeated grain boundary diffusion experiments.

Activation energies, as determined by least-square fit of the data, showed dependence on the degree of misfit. As the angle of the tilt boundary increased, the activation energy for grain boundary diffusion is shown to decrease in Figure 9. This activation energy was obtained with an assumed grain boundary width, however, as was shown, activation energy resulting from a penetration experiment is independent of width assumptions. In actuality, the assumption of constant grain boundary width for changing tilt angles in essence gives an activation energy of the diffusion parameter and not the diffusion coefficient. It must be

realized that the effective grain boundary width changes with misfit, as was shown in Turnbull and Hoffman (41). There have been attempts to determine experimentally the grain boundary width and diffusivity separately by comparison of different experiments. In general these attempts have been unsuccessful and the grain boundary diffusion coefficient is left an approximation. However, the believed increase in the grain boundary width, the increase in the diffusion parameter, $D_b\delta$, and the decrease in the activation energy for diffusion with increasing tilt angles, give strong evidence in support of diffusion occurring within dislocation pipes.

Okkerse (32) determined the grain boundary diffusivity in lead for an unspecified boundary angle. His data seemed to fit within the limits of error of this investigation for a random boundary of low misfit. The data scatter of Figure 8 and the magnitude of one standard deviation in Figure 9 demonstrate the decreasing error with large angle boundaries. The higher confidence for larger boundaries increased the accuracy of the work with varying impurities.

In this investigation of impurity content, with the exception of bismuth alloys, a general trend of decreasing penetration with increasing impurity content is noted. Lack of data for the bismuth alloys is believed attributable to the lack of adherence of the radioactive plate. When the bismuth alloys were polished with the lapping solution (1 part glacial acetic acid and 1 part 30 per cent hydrogen peroxide) a black precipitate formed. It was believed that

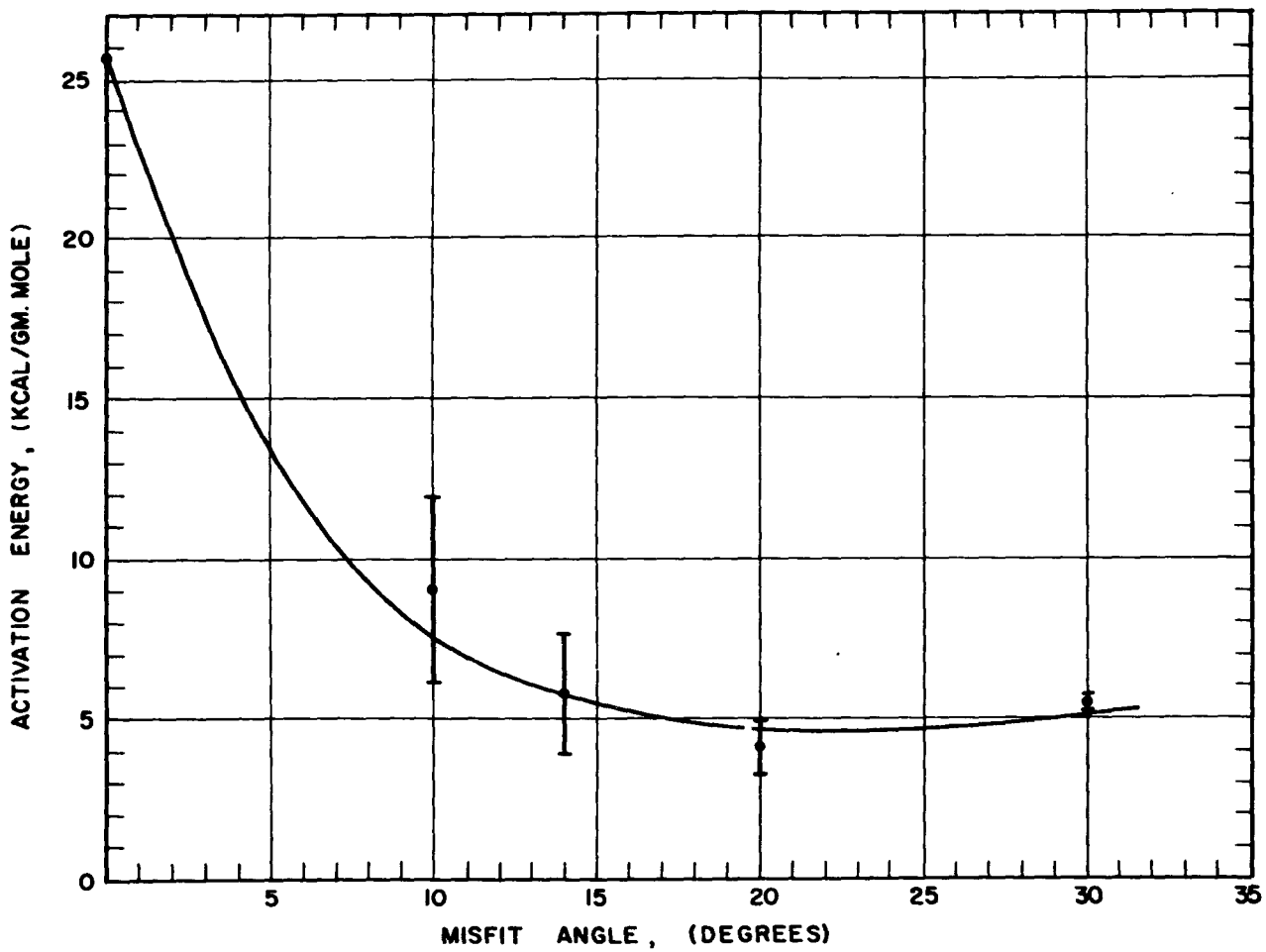

FIGURE 9. MISFIT ANGLE DEPENDENCE OF LEAD GRAIN BOUNDARY SELF-DIFFUSION ACTIVATION ENERGY.

this precipitate was bismuth trioxide (Bi_2O_3). It proved impossible to achieve a clean metallic surface with these alloys when the standard lapping solution was used. Based upon a series of evaluations, nitric acid was selected as an etchant. The results of this cleaning were still less than impressive. However, the electroplate appeared to adhere to the bismuth specimens, but no diffusion penetration was observed with the bismuth alloys.

The overall decrease in penetration with increase in alloy content was similar for each of the chosen alloying elements. From this observation, the diffusion parameter ($D_b\delta$) decreased with impurity content. Figures 10, 11, and 12 demonstrate the decrease of D_b with an assumed δ of 10^{-7} centimeters. In all cases, D_b, or more correctly $D_b\delta$, decreased an observable amount at the highest impurity content. The decrease at these concentrations was, in all cases greater than the expected experimental error of penetration. The reliability with lower alloy contents was more questionable, and these small penetration changes could be attributed to experimental error. The trend of the observed changes was, however, consistent with a linear decrease to the value associated with the maximum impurity used.

One normally expects that decreasing diffusion coefficient resulting from alloy content would produce an increased activation energy because this behavior occurs in the angle dependence. However, this change in activation

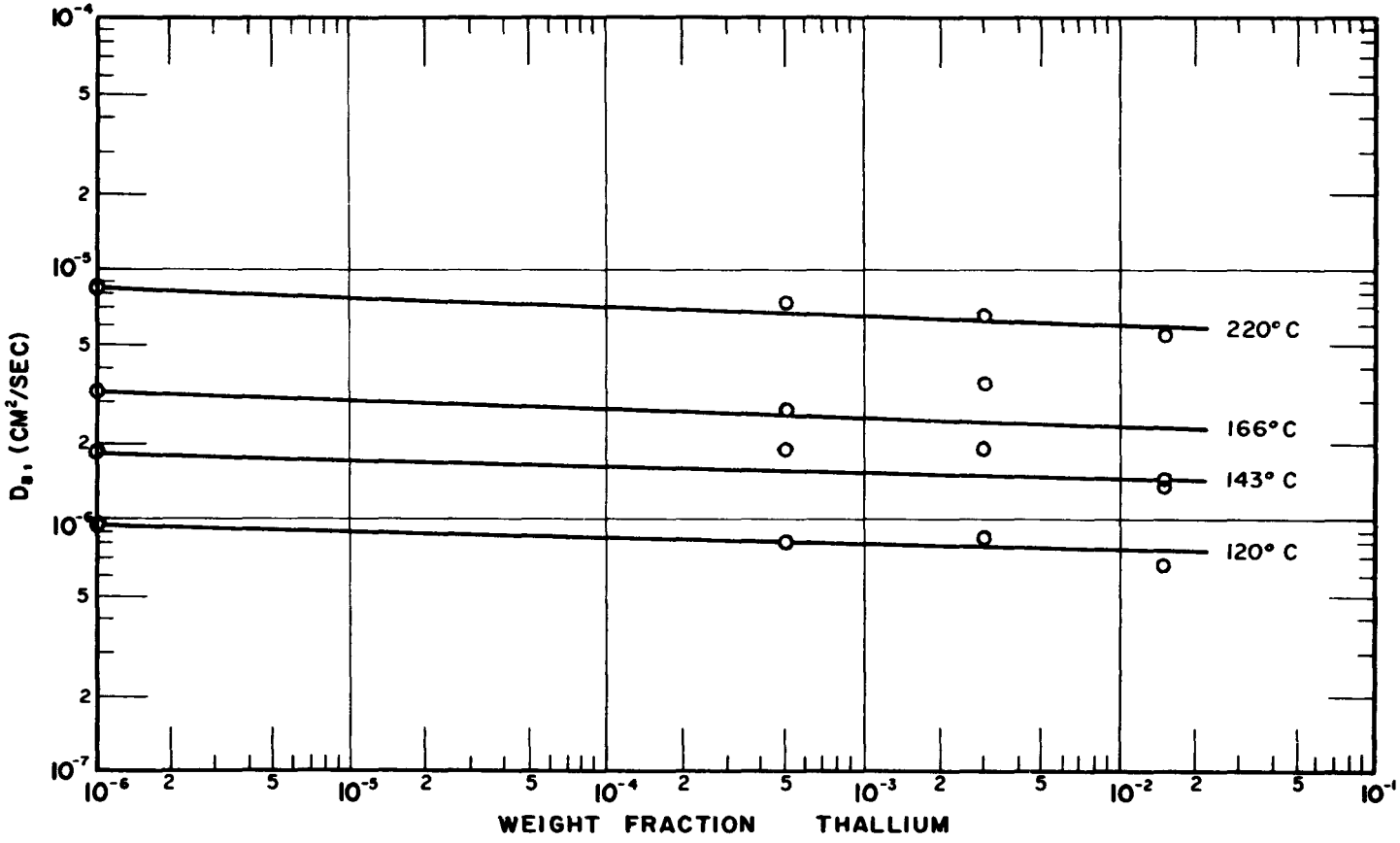

FIGURE 10. THALLIUM CONTENT DEPENDENCE OF THE GRAIN BOUNDARY SELF-DIFFUSION COEFFICIENT IN LEAD FOR A 30° MISFIT ANGLE.

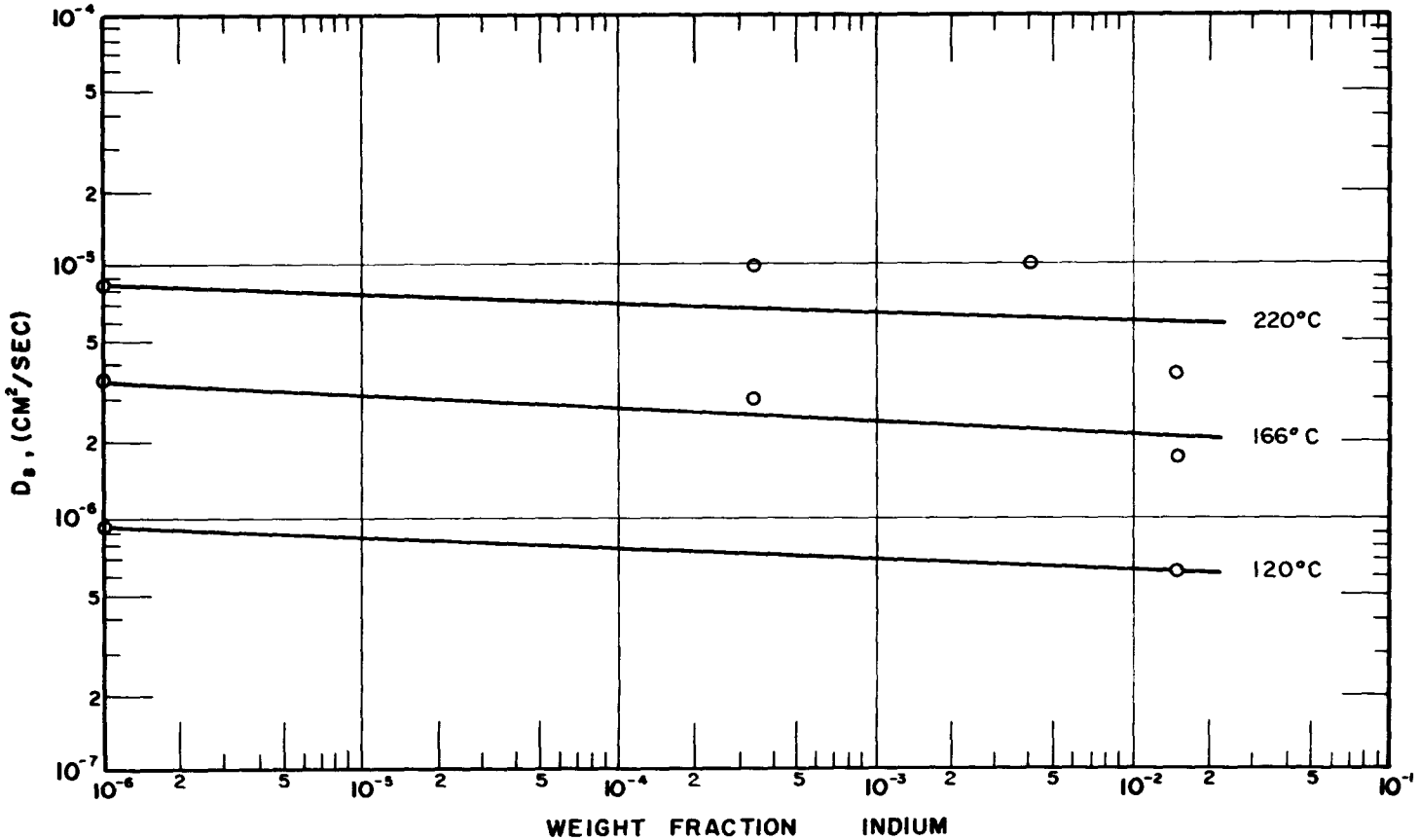

FIGURE 11. INDIUM CONTENT DEPENDENCE OF THE GRAIN BOUNDARY SELF-DIFFUSION COEFFICIENT IN LEAD FOR A 30° MISFIT ANGLE.

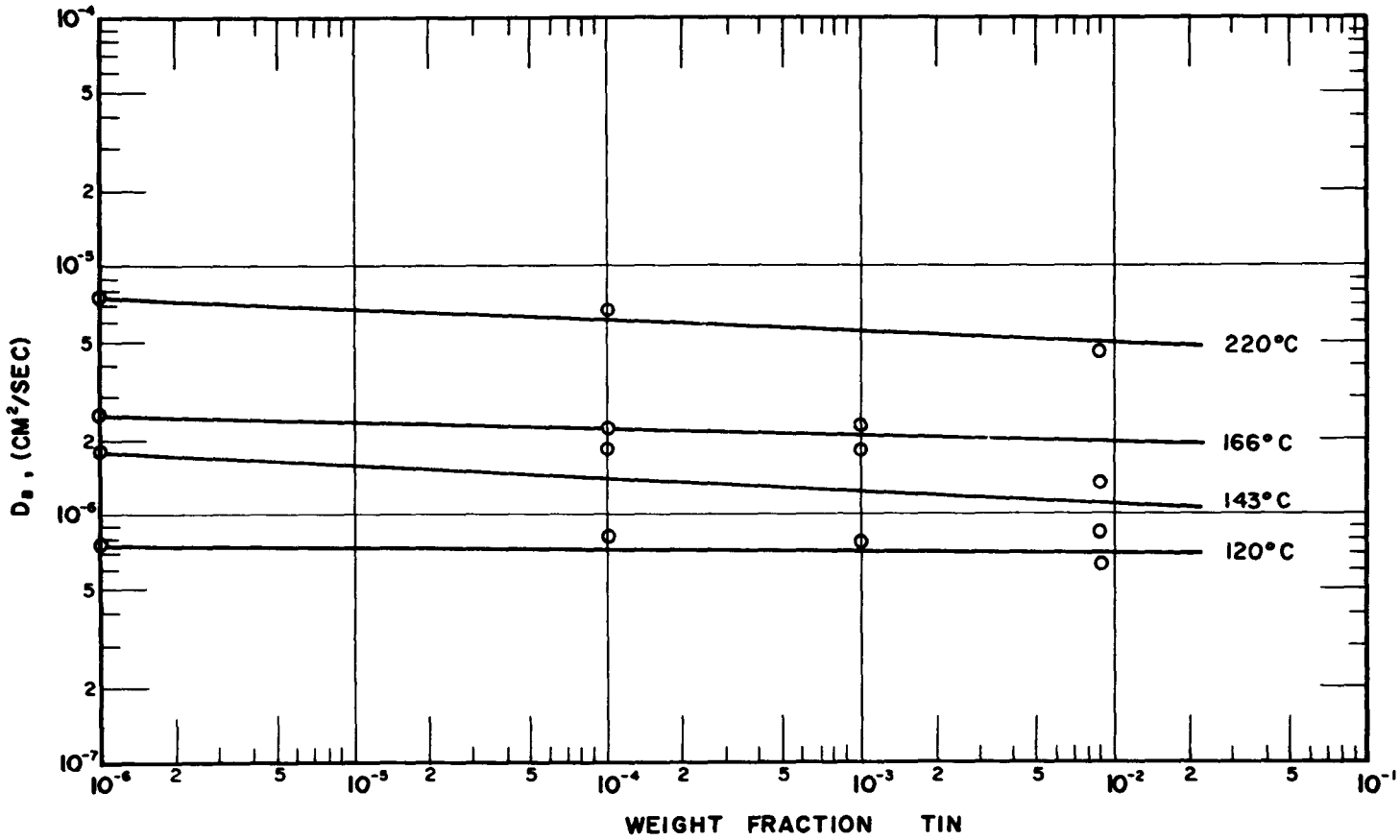

FIGURE 12. TIN CONTENT DEPENDENCE OF THE GRAIN BOUNDARY SELF-DIFFUSION COEFFICIENT IN LEAD FOR A 30° MISFIT.

energies with impurity content was not observed. Activation energies with varying impurity contents are shown for thallium and tin in Figures 13 and 14, respectively. Contrary to the supposition of increasing activation energy, a decrease was noted in both tin and thallium. Resing and Nachtrieb (37) observe a similar change in the activation energy for lattice diffusion in the lead system, the activation energy decreasing 1.6 kilocalories per gram mole from pure lead to lead with 40 per cent thallium present.

A similar change in activation energy for grain boundary diffusion was noted in indium alloys; however penetrations were often observed at two temperatures only; an example of this was 0.03 per cent indium which exhibited an activation energy of 6.6 kilocalories per mole. A least-square fit was possible with 1.5 per cent indium, and the resulting activation energy was 4.7 kilocalores per mole.

The activation energy was determined from the change of the diffusion coefficient (D_b) with temperature; the grain boundary width was assumed to be a constant 10^{-7} centimeters in these determinations. The mathematical solutions for grain boundary diffusion, as used here, actually determine the diffusion parameter ($D_b\delta$), and therefore any activation energy determined with an assumed width really represents the change of the diffusion parameter with temperature. However, the width, having a linear temperature dependence, is much less sensitive to temperature changes than is

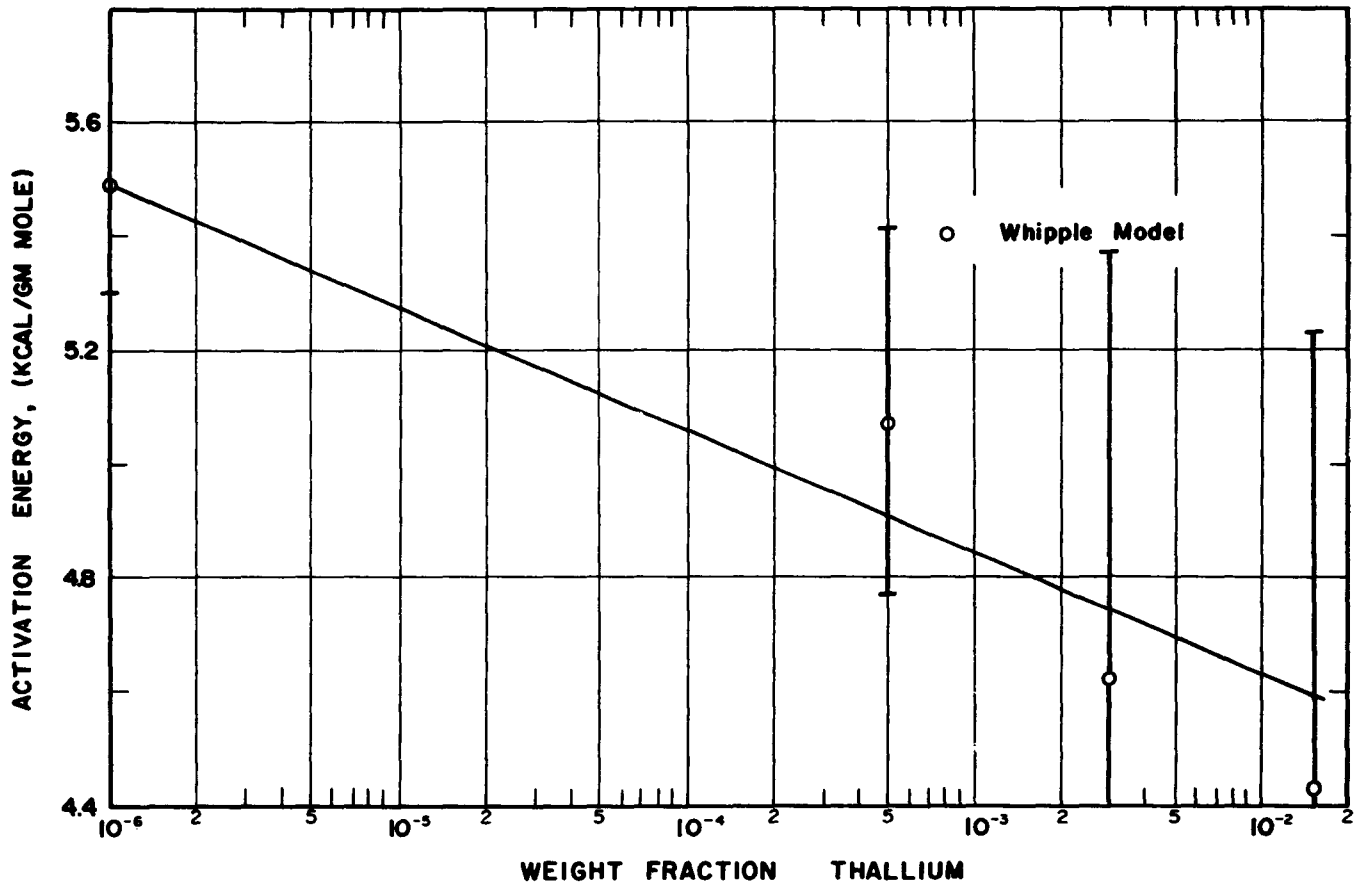

FIGURE 13. THALLIUM CONTENT DEPENDENCE OF LEAD GRAIN BOUNDARY SELF-DIFFUSION ACTIVATION ENERGY FOR A 30° MISFIT ANGLE.

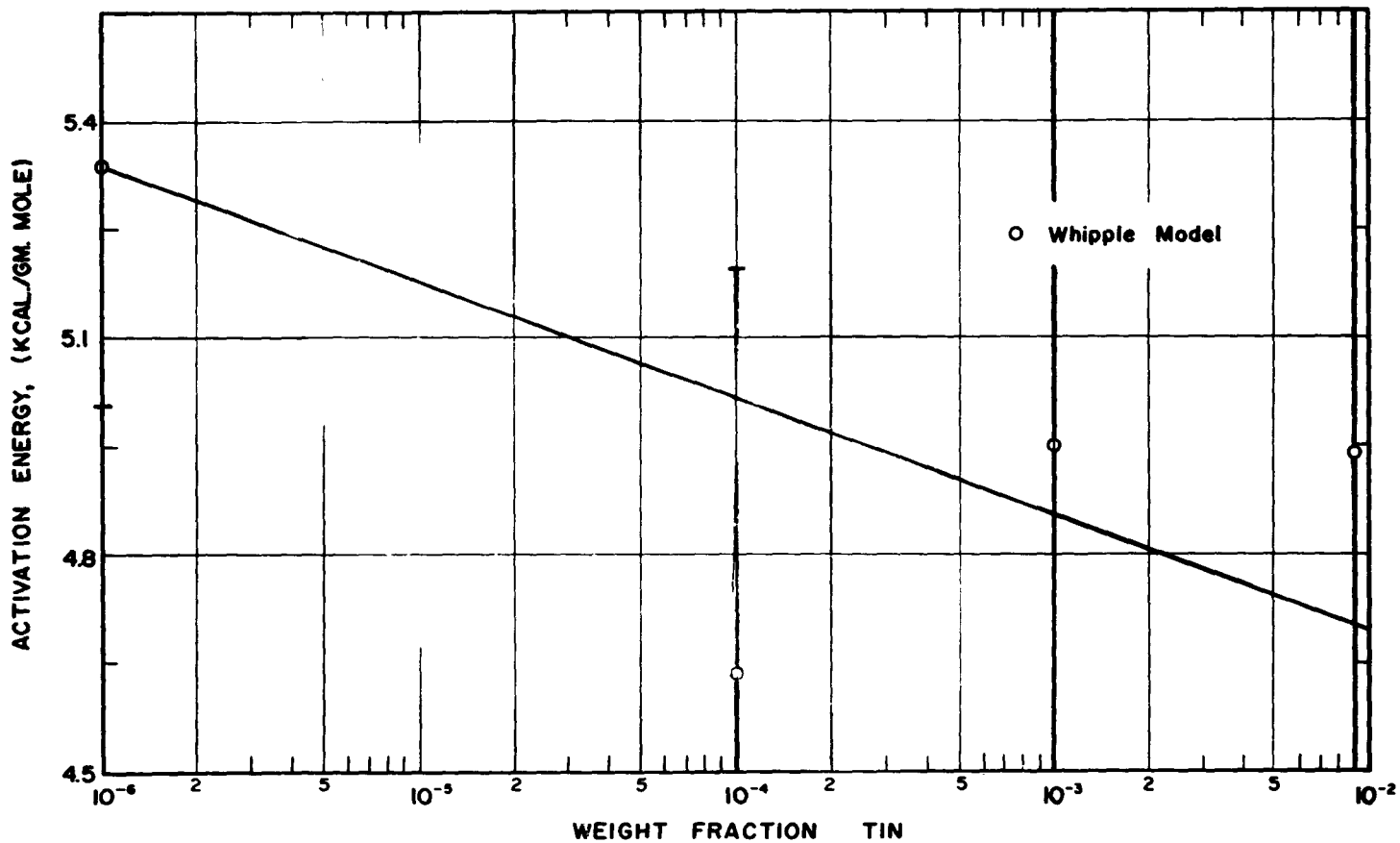

FIGURE 14. TIN CONTENT DEPENDENCE OF LEAD GRAIN BOUNDARY SELF-DIFFUSION ACTIVATION ENERGY FOR A 30° MISFIT ANGLE

diffusivity (exponential dependence). Increased impurity content decreased the diffusion parameter, but measured activation energy was rather insensitive to impurity content. The comparison of different impurity levels at a constant temperature demonstrated a 50 per cent decrease in the diffusion parameter, Figures 10, 11, and 12. Lattice diffusivity is observed to increase slightly with 20 per cent thallium present (36). Because the grain boundary width is relatively insensitive to temperature, the decreased isothermal diffusion parameter with impurity content can only be explained by a decrease in the effective width of the grain boundary. The grain boundary width, as presented in the mathematical models, has no precise physical definition. A decrease in the effective width, however, implies that the number of available diffusion paths has decreased within the grain boundary.

To test the significance of activation energy changes with impurity content, it was necessary to analyse statistically constant concentration data. The explicit results of this analysis are given in Table 13, and the method is given in Appendix B. Figure 13 clearly demonstrates that additions of thallium decreased the activation energy for grain boundary self-diffusion in a lead 30° tilt boundary. The overlap of the standard deviations of activation energy with tin additions reduces the confidence of any conclusions on this system.

One standard deviation around a mean value statistically enclosed 67 per cent of the observed data. With 0.0

TABLE 13

ACTIVATION ENERGY DEVIATION FOR VARYING MISFITS AND IMPURITY CONTENTS

Crystal Purity	Misfit	Activation Energy Kcal/mole
0.0% Tl	30° Tilt	5.56 ±0.26
0.05% Tl	30° Tilt	5.08 ±0.33
0.3% Tl	30° Tilt	4.62 ±0.81
1.5% Tl	30° Tilt	4.45 ±0.72
0.0% Sn	30° Tilt	5.36 ±0.36
0.01% Sn	30° Tilt	4.64 ±0.61
0.1% Sn	30° Tilt	4.95 ±1.21
0.9% Sn	30° Tilt	4.93 ±0.99
Pure Lead	20° Tilt	4.10 ±0.84
Pure Lead	14° Tilt	5.75 ±1.86
Pure Lead	10° Tilt	9.12 ±2.88
Pure Lead	10° Twist	8.00 ±2.56

per cent tin, the activation energy observed was 5.36 kilocalories per mole with a standard deviation of ±0.36 kilocalories per mole; however, with 0.01 per cent tin the activation energy was 4.64 ±0.61 kilocalories per mole. Another method of data analysis uses the most probable error which encloses 50 per cent of the observed data about a mean value and is 67 per cent of one standard deviation. If the tin data were analysed for most probable errors, 0.0 and 0.01 per cent tin would yield activation energies of 5.36 ±0.24 and 4.64 ±0.41 kilocalories, respectively. From this most probable error analysis, one can conclude that 0.01 per cent tin decreased the activation energy for lead grain boundary self-diffusion.

This statistical analysis gives the limits with which the data probably varies. The physical cause of this deviation as discussed earlier is the error of penetration measurements. This error was evaluated as ±0.003 centimeters, and it would represent the maximum limits of error, whereas the statistical evaluation demonstrates the probable variation.

The activation energy for grain boundary diffusion decreased with increasing amounts of impurities. Phenomenologically a decrease in activation energy for diffusion results from an increased atomic volume or possibly segregation causing a decrease in the average interatomic bond energy. Grain boundary energy has been observed by various investigators (16) and (17) to decrease with increasing impurity content. Because grain boundary energy results from a local

lattice distortion, its decrease would decrease the grain boundary energy. Impurities have been shown to cause this decrease in energy. It was previously concluded that the effective grain boundary width, as observed from diffusion, decreased with impurity content. This decrease in the effective width most certainly decreases the amount of local lattice distortion within any macroscopic grain boundary area, and this in turn would decrease the grain boundary energy. Microscopically, the amount of lattice distortion could increase or decrease in a grain boundary containing impurities; this increase or decrease would result from atomic volume changes and bond energy differences. Because the activation energy for grain boundary diffusion decreased with impurities, the strain in the immediate neighborhood of the diffusion path must have increased with a consequent reduction in the bond energy. Even though in dilute lead-tin and lead-thallium alloys the bond energy in the neighborhood of the diffusion path has decreased as compared to pure lead, the boundary width has also decreased, and from this work it is hypothesized that the grain boundary energy would decrease.

Aust and Rutter (2) have demonstrated that the free energy of activation for boundary migration and grain boundary diffusion, using the lead data of Okkerse, are about the same at the melting point. The free energy of activation is calculated from

$$\Delta F_A = Q - T\Delta S_A \ .$$

The enthalpy or energy of activation is obtained from the Arrhenius equation and the entropy of activation from D_o of the Arrhenius equation.

$$D_o = (a^2\ kT/h)\ e^{\frac{\Delta S}{R}} \qquad (16)$$

With Okkerse's data on lead grain boundary diffusion they obtain ΔF_A = 9 kilocalories per gram mole. Using the data of this investigation for a 30° grain boundary in pure lead, a value of 8.7 kilocalories per gram mole is obtained using their assumptions. Table 14 compares free energies of activation with impurity content. A value of 4 Å was used for the interatomic distance instead of their assumed 3.5 Å: the larger value deemed more appropriate for the grain boundary. Especially noteworthy in these tables is the negative entropies of activation. Also, this may be compared to the entropy of activation for liquid lead viscosity, which has been proposed to be the same as that for diffusion, and has a value of -6.27 calories per gram mole °K (44). This is very comparable to the value of -5.85 calories per gram mole °K of the 0 per cent thallium crystal.

Table 13 gives an idea of the apparent experimental error inherent in the low angle penetrations. As an example of this, the highest error in penetration occurred with the low angle boundaries at high temperatures. Due to these rather large variations in the possible values, it is felt that the activation energy with small tilt angles only tend to indicate the trend of changing misfit. The large angle

TABLE 14

FREE ENERGIES OF ACTIVATION AT 600° K FOR IMPURITY RESULTS

Compostion Wt. %	Activation Energy Kcal/gm mole	Logarithm D_o	$\frac{\Delta S}{R}$	Free Energy Kcal/gm mole
Whipple's Solution Used				
0 Tl	5.56	-6.85	-2.94	9.07
0.05 Tl	5.08	-7.55	-3.64	9.31
0.3 Tl	4.62	-8.00	-4.09	9.50
1.5 Tl	4.45	-8.62	-4.71	10.09
0 Sn	5.36	-7.27	-3.36	9.38
0.01 Sn	4.64	-8.13	-4.22	9.68
0.1 Sn	4.95	-7.77	-3.86	9.57
0.9 Sn	4.93	-8.28	-4.37	10.15
Fisher's Solution Used				
0 Tl	5.69	-7.59	-3.68	10.07
0.05 Tl	5.16	-8.33	-4.42	10.43
0.3 Tl	4.72	-8.77	-4.86	10.53
1.5 Tl	4.54	-9.37	-5.46	11.06
0 Sn	5.42	-8.06	-4.15	10.38
0.01 Sn	4.72	-8.91	-5.00	10.70
0.1 Sn	5.01	-8.57	-4.66	10.58
0.9 Sn	5.05	-9.00	-5.09	11.14

data is sufficiently more accurate and results from the decreased error in penetration measurements.

The reliability of the high angle data tends to support the small values of ln (D_o) found in Table 14. Other investigators have also noted small values. Upthegrove and Sinnott's (42) data yield values as given in Table 15.

TABLE 15

ACTIVATION ENTROPY OF NICKEL GRAIN BOUNDARY DIFFUSION

Misfit Degrees	ln Do	ΔS_A[1] Cal/Mole °K
45	-5.1	-2.1
30	-5.0	-1.9
10	-2.8	+2.5
0	-0.74	+6.6

[1]Using Equation (16) with a=2.5 Å and T=300 °K

It may be further seen in Table 15 that activation entropy changes with misfit from positive to negative values as the misfit increases. Since liquid metals show negative values of activation entropy, and lattice diffusion shows positive values, it seems feasible that the grain boundary is a transition between the positive entropies of activation for solid diffusion and the negative ones of liquids.

Diffusion is not the only process characterized with negative entropies of activation. Aust and Rutter (2) find

negative activation entropies in grain boundary migration in the lead system with and without small additions of tin with symmetrical tilt boundaries. Equation (16) could be wrong, or more likely, the negative entropy of activation for diffusion only demonstrates the relative magnitudes of configurational and vibrational entropy differences occuring in the activated state.

Fisher's equation (10) appears to be somewhat more accurate in lead high angle grain boundaries than in some other metals. A 30° grain boundary demonstrates D_b to D_L ratios lying between 10^4 and 10^8 in the temperature range 220°C to 120°C, respectively. These high ratios produce isoconcentration curves that are closely parallel to the grain boundary. The diffusion out of the grain boundary is almost perpendicular to it; this is one of Fisher's assumptions. The time variation of penetration for a 30° boundary is shown in Table 5. The slope of this time varying penetration is 0.25 from a least square fit. Fisher's theory predicts slopes of 0.25, which agrees with this value. Other researchers have obtained slopes closer to 0.33 or 0.5. These differences have been attributed to the inadequacy of Fisher's assumptions. His solution is certainly not exact, if it were, activation energies from the Whipple and Fisher solutions would be the same. Further, D_b values from the Whipple solution are 2.2 to 2.4 times greater than those from Fisher's, which is another disagreement between the two theories.

CHAPTER VI

SUMMARY AND CONCLUSIONS

Bicrystals of lead were grown with grain boundaries of controlled orientation and impurity content varying up to 1.5 per cent. The degree of perfection in these crystals was dependent upon the purity of the lead; purities above 99.99 per cent resulting in a very heavy subgrain structure. Purities less than 99.9 per cent tended to produce stray nucleation during growth; this tendancy increased with content.

Grain boundary diffusion measurements were completed with symetrical twist and tilt bicrystals with twist orientations of 4° and 10° and with tilt orientations between 3° and 30°. The extremely low angle boundaries of 3° tilt and 4° twist produced insufficient data for definite conclusions.

The grain boundary diffusion parameter ($D_b\delta$) increased with the angle of misfit in pure lead self-diffusion.

The activation energy for grain boundary diffusion decreases with increasing misfit to a limiting value of 5.46 ±0.36 kilocalories per mole for a 30° tilt angle in lead self-diffusion.

The penetration and thereby the grain boundary diffusion parameter ($D_b\delta$) decreased with increasing impurity content for the impurities tin, indium, and thallium in lead. Because the lead lattice self-diffusion coefficient is observed to increase with thallium present, the decrease in the diffusion parameter is partially attributable to a decrease in the grain boundary effective width.

There is a definite decrease in activation energy for self-diffusion with increasing thallium content. This decrease is not as pronounced in lead with tin as an impurity and inconclusive with indium. This decrease in activation energy due to the presence of impurities is compatible with grain boundary energy decreases due to impurity content because there is a decrease in the effective width.

Fisher's assumptions appear to be satisfied in time dependent penetrations for a 30° tilt boundary, but diffusivities and activation energies between Fisher's and Whipple's solutions differ in lead.

The influence of bismuth on lead grain boundary diffusion was not determinable due to lack of observed penetrations.

REFERENCES

1. Achter, M. R. and Smoluchowski, R., "Physical Review", 83,163(1951).

2. Aust, K. T. and Rutter, J. W., "Transactions of the AIME", 215,119(1959).

3. Aust, K. T. and Rutter, J. W., "Transactions of the AIME", 218,682(1960).

4. Aust, K. T. and Chalmers, B., "Proceedings of the Royal Society", 201,210(1950).

5. Austin, A. E. and Richard, N. A., "Journal of Applied Physics", 32(8),1462(1961).

6. Battner, J., Udin, K., and Wulff, J., "Journal of Metals", 5,313(1953).

7. Bolling, G. F. and Winegard, W. C., "Journal of the Institute of Metals", 86,492(1958).

8. Borisov, V. T. and Lyubov, B. I., "Fizika Metalov i Metallovedenie", 1,298(1955).

9. Bullough, R. and Newman, R. C., "Proceedings of the Royal Society", 427,227(1959).

10. Chalmers, B., "Canadian Journal of Physics", 31,132 (1953).

11. Couling, S. R. L. and Smoluchowski, R., "Journal of Applied Physics", 25,1538(1954).

12. Crussard, D., Friedel, J., and Cullity, B. D., "Acta Metallurgica", 1,79(1953).

13. Dunn, C. G. and Lionetti, F., "Journal of Metals, 1,125(1949).

14. Fisher, J. C., "Journal of Applied Physics," 22,74(1951).

15. Flanegan, R. and Smoluchowski, R., "Journal of Applied Physics", 23,785(1952).

16. Fleischer, R. L., "Acta Metallurgica", 7,817(1959).

17. Gifkins, R. C., "Transactions of the AIME", 218,1119 (1960).

18. Gjostein, J. and Rhines, S., "Acta Metallurgica", 7,319 (1959).

19. Gomberg, H., et al., University of Michigan, Report 2029--1-F, U.S. Army Ord. Corps Contract No. D A 20 018, Ord. 12150, February, 1954.

20. Gordon, P. and Vandermeer, R. A., Technical Report No. 8, Office of Naval Research Contract No. NONR 1406(03), August, 1961.

21. Gray, A. G. ed., Modern Electroplating, page 282, John Wiley and Sons, New York, 1953.

22. Guest, P. G., Numerical Methods of Curve Fitting, page 96, Cambridge, 1961.

23. Hoffman, R. E. and Turnbull, D., U.S. Atomic Energy Commission Report No. 58-RL-1883, 1958.

24. Hoffman, R. E. and Turnbull, D., "Journal of Applied Physics", 23,1409(1952).

25. Hoffman, R. E., Turnbull, D., and Hart, E. W., "Acta Metallurgica", 3,417(1955).

26. Holmes, E. L., and Winegard, W. C., "Canadian Journal of Physics", 37,899(1959).

27. Hudson, J. B. et al., Wright Air Development Center, Task No. 70645, Proj. No. 7021, Contract No. AF 33 (616)-5951, ARL Tech. Rept. 60-321.

28. Le Claire, A., Progress in Metal Physics, Vol.4, page 265 B. Chalmers, ed., Interscience Publishers Inc., New York, 1953.

29. Le Claire, D., Private Communication to W. R. Upthegrove.

30. MacKenzie, J. K., "Proceedings of the Royal Society", 63,1370(1950).

31. Nash, R. R., Office of Naval Research Technical Report ONRL-52-61, August, 1961. Meeting of Institute of Metals, London, 21-23 March, 1961 (Discussion on Segregation of Grain Boundaries).

32. Okkerse, B., "Acta Metallurgica", 2,551(1954).

33. Okkerse, B., Tiedma, T. J., and Burgers, W. G., "Acta Metallurgica", 3,310(1955).

34. Pound, G. M., Bitler, W. R., and Paxton, H. W., "Philosophical Magazine", 6,473(1961).

35. Read, W. T. and Shockley, W., "Physical Review", 75,692 (1949).

36. Read, W. T. and Shockley, W., "Physical Review", 78,275 (1950).

37. Resing, H. A. and Nachtrieb, M. H., "Journal of the Physics and Chemistry of Solids", 21,40(1961).

38. Stewart, M. T., "Physical Review", 83,657(1951).

39. Suzuoka, T., "Transactions of the Japanese Institute of Metals", 2,25(1961).

40. Thomas, W. R. and Chalmers, B., "Acta Metallurgica", 3,17(1955).

41. Turnbull, D. and Hoffman, R. E., "Acta Metallurgica", 2,419(1954).

42. Upthegrove, W. R. and Sinnott, M., "Transations of the American Society for Metals", 50,52(1957).

43. van der Merve, J. H., "Proceedings of the Physical Society", 63,313(1950).

44. Walls, H. A., Private Communication.

45. Whipple, R. T. P., "Philosophical Magazine", 45,1225 (1954).

46. Wood, V. E., Austin, A. E., and Milford, F. J., Private Communication.

47. Yukawa, S., and Sinnott, M. J., "Transactions of the AIME", 203,996(1955).

APPENDIX A

NOMENCLATURE

NOMENCLATURE

a	Lattice spacing
β	Variable in Whipple's equation
C	Concentration
δ	Grain boundary width
D_b	Grain boundary diffusivity
D_p	Dislocation pipe diffusivity
D_L	Lattice diffusivity
Δ	D_b / D_L
ξ	Variable in Whipple's equation
η	Variable in Whipple's equation
F	Free energy
$I(y)$	Unit impulse function
i	Index
j	Index
k	Index
Q	Activation energy
σ	Variable in Whipple's equation
S	Activation entropy
t	Time
x	Dimensional variable
y	Dimensional variable
z	Dimensional variable

APPENDIX B

STATISTICAL DATA ANALYSIS

STATISTICAL DATA ANALYSIS

The Arrhenius equation can be expressed in terms of logarithms, and

$$\ln D_b = \ln D_{ob} + (- \Delta H) / RT \qquad \text{B-1}$$

By substituting $U(x) = \ln D_b$, $b_o = \ln D_{ob}$, $b_1 = -\Delta H/R$, and $x = 1/T$, equation B-1 is put in the straight line form

$$U(x) = b_o + b_1 x \qquad \text{B-2}$$

If the relationship B-2 were experimentally observed, individual observations would still differ from equation B-2. Assuming a normal distribution of data points about equation B-2, a statistically probable line can be fitted to it. Any individual observation of this probable line would fit the relation

$$y_i \approx b_o + b_1 x_i$$

Equation B-2, a least square fit, is obtained after n observations, and the constants b_o and b_1 are found from Guest (22) as

$$b_1 = \{n\Sigma x_i y_i - \Sigma x_i \Sigma y_i\} / D$$
$$b_o = \{\Sigma (x_i)^2 \Sigma y_i - \Sigma x_i \Sigma x_i y_i\} / D \qquad \text{B-3}$$
$$D = n\Sigma (x_i)^2 - (\Sigma x_i)^2$$

Equations B-3 present the basis for determining diffusivities and activation energies. Because conclusions are drawn from

activation energy values, it is necessary to find the standard deviation of b_1, the slope of the line.

Using the relationship in Guest (22),

$$\sigma^2(b_1) = \sigma^2/D \qquad \text{B-4}$$

where,

$$\sigma^2 = \Sigma(y_i - U(x_i)^2/(n - 2)$$

From equation B-4, the deviation of the activation energy is obtained from

$$\sigma(\Delta H) = R\sigma(b_1) \qquad \text{B-5}$$

Table 14 presents the activation energies obtained in this investigation with their appropriate standard deviations.

The standard deviation of ln D_o or b_o is given by

$$\sigma(b_o) = \sigma\{1 + (\Sigma x_i)^2 / D\}^{\frac{1}{2}} \qquad \text{B-6}$$

This equation gives the probable variation of $\Delta S/R$, because

$$\Delta S/R = \ln D_o - \ln a^2KT/h \qquad \text{B-7}$$

From B-6 and B-7 the deviation of the entropy of activation is obtained. Therefore, for a 30° lead tilt boundary $\Delta S = -5.9 \pm 1.2$ calories per mole per degree Kelvin. This demonstrates the validity of the negative activation entropy values.

APPENDIX C

DIFFUSIVITY CALCULATION USING FISHER'S EQUATION

DIFFUSIVITY CALCULATION USING FISHER'S EQUATION

Fisher's solution as quoted in equation (9) is

$$C = C_o \exp\left[- \left(\frac{4D_L}{\pi t}\right)^{\frac{1}{2}} \frac{Y}{(D_b\delta)^{\frac{1}{2}}} \right] \left[1 - \text{erf} \left(\frac{x}{2\sqrt{D_L t}}\right) \right]$$

For a penetration measurement, $x = 0$, and the diffusion parameter $D_b\delta$ is determined from

$$D_b\delta = \{Y^2 \ (4D_L/\pi t)^{\frac{1}{2}}\} \ / \ (\ln C/C_o)^2 \qquad \text{C-1}$$

The following data apply to a 30° tilt grain boundary diffusion specimen annealed at 220° C:

$$Y = 0.062 \text{ cm},$$

$$D_L = 7.17 \times 10^{-12} \text{ cm}^2/\text{sec},$$

$$t = 3.46 \times 10^5 \text{ sec, and}$$

$$C/C_o = 10^{-5} .$$

Substituting this data into equation C-1 determined $D_b\delta$ to be 1.48×10^{-13} centimeters cubed per second. Assuming the grain boundary width is 10^{-7} centimeters,

$$D_b = 1.46 \times 10^{-6} \text{ cm}^2/\text{sec}.$$

DISTRIBUTION

Organization	No. of Copies
Chief of Naval Research Department of the Navy Washington 25, D. C. Attention: Code 423	(2)
Commanding Officer Office of Naval Research Branch Office 346 Broadway New York 13, New York	(1)
Commanding Officer Office of Naval Research Branch Office 495 Summer Street Boston 10, Massachusetts	(1)
Commanding Officer Office of Naval Research Branch Office 86 E. Randoply Street Chicago 1, Illinois	(1)
Commanding Officer Office of Naval Research Branch Office 1030 E. Green Street Pasadena 1, Cal.	(1)
Commanding Officer Office of Naval Research Branch Office 1000 Geary Street San Francisco 9, Cal.	(1)
Assistant Naval Attache for Research Office of Naval Research Branch Office, London Navy 100, Box 39 F.P.O., N.Y., N.Y.	(5)
Director U.S. Naval Research Lab. Washington 25, D. C. Attn: Technical Information Officer Code 2000 Code 2020 Code 6200 Code 6300 Code 6100	 (6) (1) (1) (2) (1)
Chief, Bureau of Naval Weapons Department of the Navy Washington 25, D. C. Attn: Code RRMA Code RREN-6	 (1) (1)
Commanding Officer U. S. Naval Air Material Cen. Philadelphia, Pennsylvania Attn: Aeronautical Materials Lab.	(1)
Superintendent U. S. Naval Weapons Factory Washington 25, D. C. Attn: Code 720	(1)
Commanding Officer U. S. Naval Ordnance Lab. White Oaks, Maryland	(1)
Commanding Officer U. S. Naval Proving Ground Dahlgren, Virginia Attn: Laboratory Div.	(1)
Chief, Bureau of Ships Department of the Navy Washington 25, D. C. Attn: Code 330 Code 337L Code 343	 (1) (1) (1)

Organization	No. of Copies
Commanding Officer U. S. Naval Engineering Experiment Station Annapolis, Maryland Attention: Metals Lab.	(1)
Materials Laboratory New York Naval Shipyard Brooklyn 1, New York Attention: Code 907	(1)
Chief, Bureau of Yards and Docks Department of the Navy Washington 25, D. C. Attention: Research and Standards Div.	(1)
Commanding Officer David Taylor Model Basin Washington 7, D. C.	(1)
Post Graduate School U. S. Naval Academy Monterey, California Attn: Dept. of Metallurgy	(1)
Office of Technical Services Department of Commerce Washington 25, D. C.	(1)
Commanding Officer U. S. Naval Ordnance Test Station Inyokern, Cal.	(1)
Armed Services Technical Information Agency (ASTIA) Documents Service Center Arlington Hall Station Arlington, Virginia	(5)
U. S. Air Force ARDC Office of Scientific Res. Washington 25, D. C. Attn: Solid State Div. (SRQB)	(1)
Commanding Officer Watertown Arsenal Watertown, Massachusetts Attn: Ordnance Materials Research Office	(1)
Laboratory Div.	(1)
Commanding Officer Office of Ordnance Research Box CM, Duke Station Duke University Durham, North Carolina Attn: Metallurgy Div.	(1)
Commander Wright Air Development Cen. Wright-Patterson Air Force Base Dayton, Ohio Attn: Aeronautical Research Lab. (WCRRH)	(1)
Aeronautical Research Lab. (WCRRL)	(1)
National Bureau of Standards Washington 25, D. C. Attn: Metallurgy Div.	(1)
Mineral Products Div.	(1)
National Aeronautics Space Administration Lewis Flight Propulsion Lab. Cleveland, Ohio Attn: Materials & Thermodynamics Div.	(1)
U. S. Atomic Energy Commission Washington 25, D. C. Attn: Technical Library	(1)
U. S. Atomic Energy Commission Washington 25, D. C. Attn: Metals and Materials Branch	(1)
Eng.Develop.Branch, Div. of Reactor Dev.	(1)

Organization	No. of Copies
Commander Wright Air Development Cen. Wright-Patterson Air Force B. Dayton, Ohio Attn: Materials Lab. (WCRTL)	(1)
Argonne National Lab. P. O. Box 299 Lemont, Illinois Attn: H.D. Young,Lib.	(1)
Brookhaven National Lab. Technical Information Div. Upton, Long Island New York Attn: Research Lib.	(1)
Union Carbide Nuclear Co. Oak Ridge National Lab. P. O. Box P Oak Ridge, Tennessee Attn: Metallurgy Div. Solid State Phys. Laboratory Records	(1) (1) (1)
Los Alamos Scientific Lab. P. O. Box 1663 Los Alamos, New Mexico Attn: Report Librian	(1)
General Electric Co. P. O. Box 100 Richland, Washington Attn: Technical Information Div.	(1)
Iowa State College P. O. Box 14A, Station A Ames, Iowa Attn: F. H. Spedding	(1)
Knolls Atomic Power Lab. P. O. Box 1072 Schenectady, New York Attn: Document Lib.	(1)
U. S. Atomic Energy Com. New York Operations Office 70 Columbus Avenue New York 23, New York Attn: Document Custodian	(1)
Sandia Corporation Sandia Base Albuquerque, New Mexico Attn: Library	(1)
U. S. Atomic Energy Com. Technical Information Service Extension P. O. Box 62 Oakridge, Tennessee Attn: Reference Branch	(1)
University of California Radiation Laboratory Information Division Room 128, Building 50 Berkeley, California Attn: R. K. Wakerling	(1)
Bettis Plant U. S. Atomic Energy Com. Bettis Field P. O. Box 1468 Pittsburgh 30, Pennsylvania Attn: Mrs. Virginia Sternberg, Librarian	(1)
Commanding Officer & Director U. S. Naval Civil Engr. Lab. Port Hueneme, Cal.	(1)
Commanding Officer U. S. Naval Ordnance Underwater Station Newport, Rhode Island	(1)
U. S. Bureau of Mines Washington 25, D. C. Attn: Dr. E. T. Hayes	(1)

Organization	No. of Copies
Defense Metals Information Center Battelle Memorial Institute 505 King Avenue Columbus, Ohio	(2)
Solid State Devices Branch Evans Signal Laboratory U. S. Army Signal Engr. Labs. c/o Senior Navy Liaison Off. Fort Monmouth, New Jersey	
U. S. Bureau of Mines P. O. Drawer B Boulder City, Nevada Attn: Electro-Metallurgical Div.	(1)
Commanding General U. S. Army Ordnance Arsenal, Frankford Philadelphia 37, Pa. Attn: Mr. Harold Markus ORDBA-1320, 64-4	(1)
Prof. E. R. Parker Div. of Mineral Technology University of California Berkeley 4, Cal.	(1)
Prof. W. A. Backofen Dept. of Metallurgy Mass. I. of T. Cambridge 39, Mass.	(1)
Dr. M. Gensamer Dept. of Metallurgy Columbia University New York 27, New York	(1)
Prof. B. Chalmers Dept. of Engr. & Applied Physics Harvard University Cambridge, Mass.	(1)
Prof. N. Brown Univ. of Pennsylvania Dept. of Metallurgical Engr. Philadelphia 4, Pennsylvania	(1)
Dr. R. Maddin Dept. of Metallurgy Univ. of Pennsylvania Philadelphia 4, Pa.	(1)
Prof. M. E. Fine Dept. of Metallurgy Northwestern Univ. Evanston, Illinois	(1)
Dr. J. A. Sabato Metallurgy Division Comision Nacional de Energia Atomica Buenos Aires Argentina	(1)
Dr. H. M. Otte RIAS Division Martin-Marietta Corp. Baltimore, Maryland	(1)
Dr. S. Weissmann College of Engineering Rutgers University New Brunswick, N. J.	(1)
Prof. R. A. Huggins Dept. of Metallurgical Engr. Stanford University Standard, Cal.	(1)
Prof. D. N. Beshers School of Mines Columbia University New York 27, N. Y.	(1)
Prof. J. W. Kauffmann Dept. of Metallurgy Northwestern University Evanston, Illinois	(1)

Organization	No. of Copies
Dr. H. G. F. Wilsdorf Franklin Institute Benjamin Franklin Parkway at 20th St. Philadelphia 3, Pa.	(1)
Dr. R. E. Maringer Battelle Memorial Institute 505 King Avenue Columbus 1, Ohio	
Prof. I. Cadoff Department of Metallurgical Engr. New York University University Heights New York 53, N. Y.	(1)
Prof. R. B. Gordon Dept. of Metallurgy Yale University New Haven, Conn.	(1)
Prof. C. Elbaum Metals Research Lab. Brown University Providence 12, Rhode I.	(1)
Dr. T. Vreeland Cal. Inst. of Technology Dept. of Mechanical Engr. Pasadena, Cal.	(1)
Prof. C. W. Allen Dept. of Metallurgy University of Notre Dame Notre Dame, Indiana	(1)
Prof. B. D. Cullity Dept. of Metallurgy University of Notre Dame Notre Dame, Indiana	(1)
Prof. J. B. Cohen Dept. of Materials Sc. Northwestern University Evanston, Illinois	
Prof. J. J. Gilman Division of Engineering Brown University Providence, R. I.	(1)
Prof. O. D. Sherby Division of Materials Sc. Stanford University Stanford, Cal.	(1)
Dr. G. S. Ansell Rensselaer Polytechnic Inst. Troy, New York	(1)
Dr. H. Peiffer RIAS 7212 Bellona Avenue Baltimore, Maryland	(1)
Prof. F. Seitz Department of Physics University of Illinois Urbana, Illinois	(1)
Prof. T. A. Read Dept. of Mining & Met. Engr. University of Illinois Urbana, Illinois	(1)
Prof. R. Smoluchowski Dept. of Mechanical Engr. Princeton University Princeton, New Jersey	(1)
Dr. A. E. Austin Battelle Memorial Institute 505 King Avenue Columbus 1, Ohio	(1)
Prof. H. Brooks Dean of Graduate School of Applied Science Harvard University Cambridge, Massachusetts	(1)
Prof. H. B. Huntington Dept. of Physics Rensselaer Polytechnic Inst. Troy, New York	(1)

Organization	No. of Copies
Prof. J. S. Koehler Dept. of Physics University of Illinois Urbana, Illinois	(1)
Prof. E. Orowan Dept. of Mech. Engr. Mass. Inst. of Tech. Cambridge 39, Mass.	(1)
Prof. Vernon Griffiths Montana School of Mines Butte, Montana	(1)
Dr. M. J. Donachie Electric Boat Division General Dynamics Corp. Groton, Conn.	(1)
Prof. M. J. Sinnott University of Michigan Ann Arbor, Michigan	(1)